SERI/STR-211-2637
(DE85008804)

PHOTOVOLTAIC DEVICES USING a-Si:H FROM HIGHER ORDER SILANES

By
A. E. Delahoy

March 1985

Work Performed Under Contract No. AC02-83CH10093

Chronar Corporation
Princeton, New Jersey

and

Solar Energy Research Institute
Golden, Colorado

Technical Information Center
Office of Scientific and Technical Information
United States Department of Energy

DISCLAIMER

Available from the National Technical Information Service, U. S. Department of Commerce, Springfield, Virginia 22161.

Price: Printed Copy A04
Microfiche A01

Codes are used for pricing all publications. The code is determined by the number of pages in the publication. Information pertaining to the pricing codes can be found in the current issues of the following publications, which are generally available in most libraries: *Energy Research Abstracts (ERA); Government Reports Announcements* and Index *(GRA* and I); *Scientific and Technical Abstract Reports (STAR);* and publication NTIS-PR-360 available from NTIS at the above address.

Printed in the United States of America
USDOE Office of Scientific and Technical Information
Oak Ridge, Tennessee

SERI/STR-211-2637
(DE85008804)
Distribution Category UC-63

Photovoltaic Devices Using a-Si:H from Higher Order Silanes

Final Subcontract Report
September 1, 1983 - August 31, 1984

A. E. Delahoy

Chronar Corporation
Princeton, New Jersey

March 1985

Prepared under Subcontract No. XL-3-03147-1

SERI Technical Monitor: Byron Stafford

Solar Energy Research Institute
A Division of Midwest Research Institute

1617 Cole Boulevard
Golden, Colorado 80401

Prepared for the
U.S. Department of Energy
Contract No. DE-AC02-83CH10093

PREFACE

This report describes the preparation of hydrogenated amorphous silicon (a-Si:H) films and photovoltaic devices by chemical vapor deposition (CVD) from higher silanes, and the properties of such films and devices. The motivation for this research is the prospect of preparing by a new technique a-Si:H having electronic properties similar (or superior) to material prepared by the well-known glow discharge technique. Possible advantages of thermal CVD are the absence of ion bombardment, high deposition rates, efficient utilization of feedstock gases, lower levels of impurity incorporation, absence of pinholes, and greater material stability. Photochemical vapor deposition of a-Si:H from disilane is also described and has yielded higher efficiency solar cells than thermal CVD.

The research was performed by;

A.E. Delahoy	Principal Investigator/Program Manager
F.B. Ellis	Scientist
A. Vaseashta	Research Associate
T. Rotberg	Technician
B. Doele	Technician
J. Van Dine	Technician

I am indebted to my colleagues Dr. M. Akhtar and Mr. A. Lichter for the in-house preparation of higher silanes of exceptional purity and their analysis by gas chromatography. The ITO evaporations were performed by Mr. J. Houghton. Thanks are also due to Dr. W.E. Carlos (Naval Research Laboratory) for ESR measurements, Dr. W.A. Lanford (SUNY) for the nuclear reaction analysis, Dr. R.R. Corderman (Brookhaven National Laboratory) for modulated beam mass spectrometry, Dr. T. McMahon (SERI) for surface photovoltage measurements, and Mr. J. Dick (SERI) for the SIMS analyses.

SUMMARY

Research performed under subcontract No. XL-3-03147-1 ("Photovoltaic Devices Using a-Si:H From Higher Order Silanes") for the twelve month period 9/1/83 - 8/31/84 is described. The work is summarized in this section under the heading Objectives, Discussions and Conclusions.

Objectives The program objectives are to continue characterization and development of a-Si:H prepared by CVD using higher order silanes. Deposition conditions will be varied to optimize doped and undoped layers. The quality of the films will be evaluated by fabrication of Schottky barrier and p-i-n devices, and by other optoelectronic techniques. Specific goals include a method for measuring carrier diffusion length, the attainment of a short-circuit current density of 9mA cm^{-2}, and a conversion efficiency of 5%.

Discussion Hydrogenated amorphous silicon was prepared by chemical vapor deposition from higher silanes using flow methods rather than a static method in order to deposit from a time-invariant gas-phase chemistry. Electronic grade higher silanes were manufactured at Chronar by subjecting CCD grade monosilane to a silent electric discharge (SED). A typical analysis of the higher silanes by gas chromatography indicated 35% SiH_4 61% Si_2H_6, 4.4% Si_3H_8, and 0.4% H_2; oxysilanes, chlorosilanes, and hydrocarbons were undetectable. Low pressure CVD, atmospheric pressure CVD, and, later in the program, mercury sensitized photo-CVD systems were employed, with deposition rates typically being 10Å s^{-1}, 15-20 Å s^{-1}, and 0.2 Å s^{-1} respectively.

Films prepared by LPCVD at 470 °C have an optical band gap of 1.67 eV and a bulk spin density of 1 x 10^{17} cm^{-3}. Films prepared by APCVD at 435 °C have a band gap of 1.72 eV, and a hydrogen content of 16-17%. Both types of film are photoconductive, but the AM1 photoconductivity of each is generally less than 5 x 10^{-6} ohm^{-1} cm^{-1}.

Films prepared by photo-CVD have a band gap of 1.8 eV and an AM1 photoconductivity greater than 1 x 10^{-5} ohm^{-1} cm^{-1}. The temperature dependence of the photoconductivity of photo-CVD i layers exhibits a low temperature peak and thermal quenching between 125-200 K. SIMS analysis reveals lower levels of the impurities C, O, N, Cl in LPCVD a-Si:H (prepared using SED disilane) than in glow discharge a-Si:H. Atmospheric impurities (O, N) in photo- CVD films are comparable to those in glow discharge films.

Systematic variation of deposition parameters such as pressure, flow rate, etc. were made for a standard Au/i-n^+/metal substrate Schottky device in both LPCVD and

APCVD systems, with photovoltaic performance being used as the principal judge of i layer quality. Both LPCVD and APCVD Schottky devices finally attained AM1 conversion efficiencies of 1.2%. A graded ppm boron doping of the i layer in APCVD Schottky devices resulted in an external AM1 short circuit current density of 5.5 mA cm^{-2}. By contrast, the very first photo-CVD Schottky devices attained an efficiency of 2.0% and a current density of 7.4 mA cm^{-2} (illuminated through SnO_2 rather than Au).

Conscious of the historically poor performance of CVD p layers in p-i-n devices a considerable effort was expended to develop a higher quality LPCVD p layer. The parameters which were varied were: the composition of the gas-phase reactants (including monosilane, disilane, trisilane, diborane, and acetylene), the temperature (170 - 470 °C), the pressure (1 - 50 Torr), and the reactant flow rates (0.2 - 90 sccm). Two types of wide band gap (window) p layers were obtained. Remarkably, one type of boron doped a-Si:H window layer can be prepared at low temperatures (200 - 300 °C) from diborane/trisilane mixtures. It has a band gap of about 2 eV, a dark conductivity of 5 x 10^{-7} ohm^{-1} cm^{-1}, an activation energy of 0.37 eV, and 26 atomic % hydrogen. The second type of window layer is a silicon-carbon alloy having a similar band gap, conductivity and activation energy, but is prepared at high temperatures (470 °C).

PIN devices prepared by LPCVD, and having the structure ITO/p-i-n/metal substrate where the p layer is the low temperature window layer just described, exhibited open circuit voltages up to 723 mV and short circuit current densities up to 10.0 mA cm^{-2}. Device efficiency was found to be sensitive to the initial distribution of higher silanes in the gas mixture. In particular, it was found that the presence of trisilane during deposition of the p layer leads to higher voltages, and that dilution of the higher silane mixture with monosilane during the deposition of the i-layer improves the fill factor. The highest efficiency obtained was 3.1%.

PIN devices prepared by photo-CVD with the structure Al/n-i-p/SnO_2/glass substrate have exhibited current densities up to 10.1 mA cm^{-2}, and interestingly enough, fill factors greater than 0.66. The highest efficiency obtained during the contract was 4.4%.

A set-up for the measurement of collection length Lco (the sum of electron and hole drift lengths) was devised and from these measurements the diffusion length in LPCVD and photo-CVD a-Si:H was calculated. In this way diffusion lengths of 0.1 μm and 0.12 μm were obtained for the two types of material.

Conclusions It has been demonstrated that flow CVD techniques are capable of higher (single junction) device efficiencies than the static CVD method employed in previous contracts. As a result of the adoption of flow methods, together with systematic optimization and the use of high purity SED disilane, the electronic properties of a-Si:H prepared by thermal CVD have been substantially improved. Of considerable interest is the development of a radically improved LPCVD p layer, a window layer prepared at low temperatures from diborane and trisilane. However, despite considerable efforts, LPCVD device efficiencies never exceeded 3.1%, whereas photo-CVD efficiencies quickly reached 4.4%. The inferior properties of LPCVD cells cannot be ascribed to common impurities such as C, O, N, or Cl (since use of SED disilane results in very low concentrations of these impurities), but is rather probably connected with the habitually low photoconductivity ($<5 \times 10^{-6}$ ohm^{-1} cm^{-1} at AM1). This results in poor fill factors. The low photoconductivity is a consequence of a relatively high (and possibly unavoidable) density of dangling bonds (1×10^{17} cm^{-3}) that shorten the electron lifetime. On the other hand, a-Si:H prepared by photo-CVD has a higher photoconductivity and devices usually have excellent fill factors. There does not appear to be any reason why a 10% efficient cell could not be made by photo-CVD.

TABLE OF CONTENTS

LIST OF FIGURES

Page

LIST OF TABLES

Page

ABSTRACT

This report describes the preparation of hydrogenated amorphous silicon (a-si:H) films and photovoltaic devices by chemical vapor deposition (CVD) from higher silanes and lists the properties of such films and devices. The motivation for this research is the prospect of preparing, by a new technique, a-Si:H having electronic properties similar to or superior to material prepared by the well-known glow discharge technique. Possible advantages of thermal CVD are the absence of ion bombardment, high deposition rates, efficient utilization of feedstock gases, lower levels of impurity incorporation, absence of pinholes, and greater material stability. Photochemical vapor deposition of a-Si:H from disilane is also described and has yielded higher efficiency solar cells than thermal CVD.

SECTION 1
INTRODUCTION

1.1 DEPOSITION METHODS

Under our previous contracts (XL-2-02181-1 and XG-1-12421-1) hydrogenated amorphous silicon was prepared from higher order silanes by a static CVD method. This method involves admitting the silane mixture into the deposition chamber until a predetermined pressure is attained, and then isolating the chamber until the required thickness of a-Si:H is grown on the heated substrate. A conversion efficiency of 1.4% was obtained for a single-junction p-i-n device, and 4% for a three-stack (pinpinpin) devices. Largely based on this work, a fairly detailed analysis of the properties of a-Si:H prepared by static CVD was published [1].

In our present contract we have turned our attention to flow CVD methods, for the following reasons. In CVD both homogeneous gas phase and heterogeneous gas-surface reactions can be important. At the beginning of the CVD process the reactants start breaking up and the process is fairly simple. However, as the CVD process continues complicated new species are generated which can be important in determining the properties of the deposited material. Still later in the CVD process the chemistry becomes less complicated in the sense that most of the reactants have been consumed and stable products and by-products have been formed. In the static method all these vastly changing reaction conditions contribute to the film deposition. Even in the step-static method developed in the last contract, in which the deposition chamber is evacuated and refilled with disilane three or four times during the deposition in order to limit the extent of reaction, SIMS analysis confirmed that hydrogen and oxygen concentrations in the film varied in a sawtooth fashion corresponding to the changing deposition chemistry during each deposition step. By contrast, in laminar flow CVD methods it is possible to deposit the film at a given extent of reaction by altering the temperature and flow rate. In other words, the entire deposition can occur under optimum conditions.

For the present contract we therefore proposed to prepare a-Si:H films and devices by a) laminar flow atmospheric pressure CVD, b) low pressure flow CVD, and based on some encouraging results from mercury-sensitized decomposition of disilane [2], by c) photo-CVD. In order to properly assess the quality of i-layer material it was decided that device work would be restricted to single-junction devices.

1.2 PURITY OF HIGHER SILANES

Most of the work performed under our last contract was performed with disilane prepared by a chemical process, namely the reaction of Mg_2Si with HCl or H_3PO_4 followed by trap to trap distillation. Under the present contract higher silanes manufactured at Chronar by subjecting CCD grade monosilane to a silent electric discharge (SED) have been used. It has been verified that this source gas is exceptionally pure.

SECTION 2
TECHNICAL DISCUSSION

2.1 TASK 1: MATERIAL PREPARATION AND ANALYSIS

The design of the deposition systems for the three proposed CVD methods (LPCVD, APCVD and photo-CVD) and the properties of the resulting a-Si:H films will be discussed separately for each method in subsections 2.1.2 - 2.1.4.

2.1.1 Disilane Analysis

The composition of the higher silane feedstock gas used in this work was analyzed by gas chromatography. A typical analysis indicates :

35% SiH_4
61% Si_2H_6
4.4% Si_3H_8
0.4% H_2

No oxysilanes or chlorosilanes were detected. Using a column appropriate for the detection of hydrocarbons, neither were any hydrocarbons detected (sensitivity 1 ppm), nor were CO_2, O_2, N_2, or nitrogen oxides detected (sensitivity 10 ppm). Upon analysis of a similar sample of SED disilane by modulated beam mass spectrometry, oxysilanes were detected at the very low level of 67 ppm. Again, no chlorosilanes or hydrocarbons could be detected. It is estimated that the sensitivity for chlorosilanes by this technique is of the order of 1 ppm. From these analyses we conclude that the SED disilane is of very high purity and may be termed "electronic grade". Moreover, it seems likely that the properties of a-Si:H films prepared by CVD from this gas are determined solely by the relative concentrations of the silanes and by other deposition parameters, and are not influenced by gaseous impurities since they are practically absent.

Disilane was also procured from a Japanese producer (Mitsui Toatsu) and analyzed at Chronar by gas chromatography. Assuming equal response factors the analysis showed:

2.1% monosilane
96.7% disilane
0.7% trisilane
0.5% other (presumably mostly chlorosilanes, since elution time slightly longer than for disilane).

Compared to Chronar's higher silane gas produced by SED this gas is notable for the absence of significant quantities of trisilane and still higher silanes. While the gases appear to be of comparable quality regarding impurities, the difference in higher silane distribution is a major difference.

2.1.2 Low Pressure CVD (LPCVD)

The deposition system used for LPCVD from higher silanes is shown schematically in Figure 1. It is based on a cylindrical stainless steel chamber containing a smaller diameter re-entrant cylinder with an end plate that supports the substrates. The end plate is heated from the air side of the system, while the chamber itself is heated by an external heating jacket. The deposition and properties of i layers, p layers, and n layers are discussed below.

2.1.2.1 I Layer Studies

The basic properties of LPCVD a-Si:H i layers are as follows. The energy gap as determined by the conventional $(\alpha E)^{1/2}$ versus E plot, is 1.67 eV for a substrate temperature Ts of 470 °C. The AM1 photoconductivity ranges from 8×10^{-7} ohm^{-1}cm^{-1} to 5×10^{-6} ohm^{-1}cm^{-1}. Typical films deposited at 470 °C and at a pressure of 20 Torr (deposition rate 10Å s^{-1}) possess a bulk spin density of the order of 10^{17} cm^{-3} as determined by etch-back experiments and ESR at the Naval Research Laboratory. The resonance was obtained at the usual g= 2.0055 value. The surface density of spins rises to two to three times that value. The measured spin densities are therefore given in Table 1 as a surface density.

TABLE 1 Spin density of LPCVD films as a function of thickness.

Sample	Substrate Temperature (°C)	Thickness (μm)	Spins cm^{-2} (x 10^{14})
746	470	0.5	0.3
745	470	1.0	0.5
747	470	2.0	0.9

Surface photovoltage measurements made on thick i-n$^+$ LPCVD a-Si:H films supplied to SERI yielded effective diffusion lengths of 0.35 μm (dark) and 0.15 μm (AM1).

For CVD to be a competitive technique for the production of a-Si:H solar cells, a much lower density of defect states in the energy gap is required. For example, because of the 1×10^{17} cm^{-3} spin density the photoconductivity is lower than that needed for high efficiency cells. Also, because of high deposition temperatures (generally, greater than 400 °C), contamination of

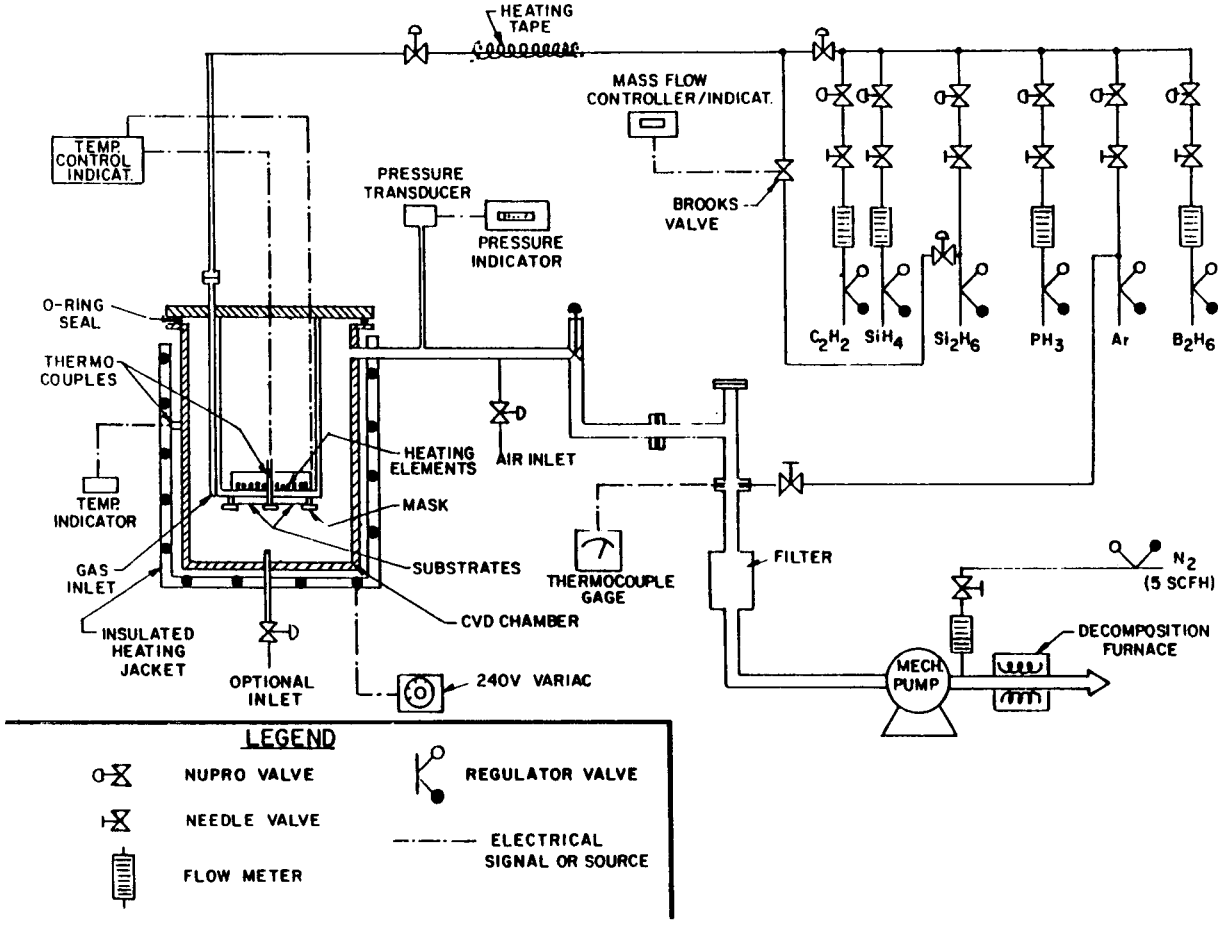

Fig. 1. Schematic diagram of low pressure CVD (LPCVD) system.

the film by diffusion of species across the film/substrate interface can be a major concern. Thus in directly depositing on tin oxide the strong oxidation-reduction reaction between tin oxide and a-Si:H results in both a highly contaminated a-Si:H film and tin oxide film. A standard substrate for much of the work on LPCVD and APCVD presented below was stainless steel (ss). Even for this substrate SIMS analyses provided by SERI show the diffusion of species (including chromium and iron) across the a-Si:H/ss interface. (However, there is no firm evidence of lower device efficiencies resulting from this diffusion provided a 2000 Å thick n layer is used). By means of appropriate diffusion barriers, work is in progress to assess the degradation of the a-Si:H by substrate contamination.

Another area of interest concerns the distribution of higher silanes in the feedstock gas mixture. Use of optimal deposition conditions established for our SED gas with the Japanese (Mitsui Toatsu) gas led to a film growth rate about an order of magnitude lower. It was suspected and confirmed that without a significant amount of trisilane (see section 2.1.1, Disilane Analysis) a longer gas-phase residence time is needed to develop a similar gas-phase chemistry. Hence, for example, by reducing the total flow rate of 12.7 sccm for the SED gas to 2.6 sccm for the Japanese gas most of the former growth rate was recovered.

2.1.2.2 P Layer Studies

We report our results for the chemical vapor deposition of various boron doped hydrogenated amorphous silicon (p a-Si:H) and silicon-carbon alloy (p a-Si_xC_{1-x}:H) layers. Our objective has been to achieve a suitable CVD p layer for use in a-Si:H solar cells. Two types of window layers are obtained. One is deposited at low temperatures (200-300 °C), where the large optical band gap stems from a high hydrogen concentration. The other is a silicon-carbon alloy where the source of carbon is acetylene. However, only the wide band gap material without carbon appears suitable for photovoltaic devices.

The basic parameters of interest in this study consist of the composition of the gas-phase reactants (including monosilane, disilane, trisilane, and acetylene), the temperature (170-470 °C), the pressure (1-50 torr), and the reactant flow rates (0.2-90 cc/min) from which the gas-phase residence time and reactant ratios can be determined. The p layers are characterized by device performance, Auger and SIMS analysis, optical properties, dark conductivity, and the thermal activation energy of the dark conductivity (slope of an Arrhenius plot).

M. Hirose et al. reported boron and phosphorus doped films produced by the CVD of monosilane containing diborane and phosphine respectively [3]. They observed that diborane had a catalytic effect on the decomposition of the monosilane. In these experiments a deposition temperature of 550 °C was used. This

temperature was about 100 °C lower than that used in the phosphine-monosilane mixture [3]. Others have briefly mentioned CVD p layers using higher order silanes [1, 4, 5].

We have made material from monosilane-diborane mixtures at 470 °C where the dark conductivity exceeds 10^{-2} $(ohm\text{-}cm)^{-1}$. Unfortunately, this material is strongly absorbing in visible light (see Figure 2 sample #785). Furthermore, in CVD devices, the use of this material for the p layer results in a low open-circuit voltage (Voc) of about 0.4 volts (see Table 2). Since the deposition time of the p layer is short and since the device is immediately cooled after the p layer is deposited, boron diffusion is not expected to be the cause of the low Voc. The Voc is related to the difference between the Fermi levels in the n and p layers. Therefore, a possible explanation for the low Voc is that this difference has been made smaller by the shifting of the valence band edge closer to the vacuum level in this narrow band gap material (see Figure 3). From Auger analysis, this material is really a silicon-boron alloy since the boron concentration can be comparable to the silicon concentration.

In an attempt to reduce the excessive boron concentration found in films deposited from monosilane-diborane mixtures, higher order silanes were used. A study of the decomposition of disilane and diborane mixtures done at 200 °C reveals that it is possible to deposit principally hydrogenated silicon. At this temperature the deposition of species is initiated only by the decomposition of diborane. Presumably, the diborane decomposes into BH_3 radicals, some of which react with disilane to produce silicon-containing radicals which can undergo further reaction in the gas phase. As these radicals strike the substrate surface there is a high probability that they add to or bond to the surface producing film growth and possibly a reactive surface for further gas-surface heterogeneous reactions. Whatever the mechanism, the resulting films have been measured by Auger analysis to have a boron/silicon ratio about seven to ten times greater than the initial gas-phase ratio. However, because of the weak dependence of the growth rate on the diborane concentration,* we are able to deposit films where the boron concentration is below the Auger detection limit (less than one atomic percent). Quantitative SIMS analysis of sample #935 (see Table 3) shows 0.4-0.5 atomic percent boron.

---

* For the experimental conditions used at 200 °C, the film growth rate is approximately proportional to $[Si_2H_6]_o^{0.3}$ $[B_2H_6]_o^{0.6}$.

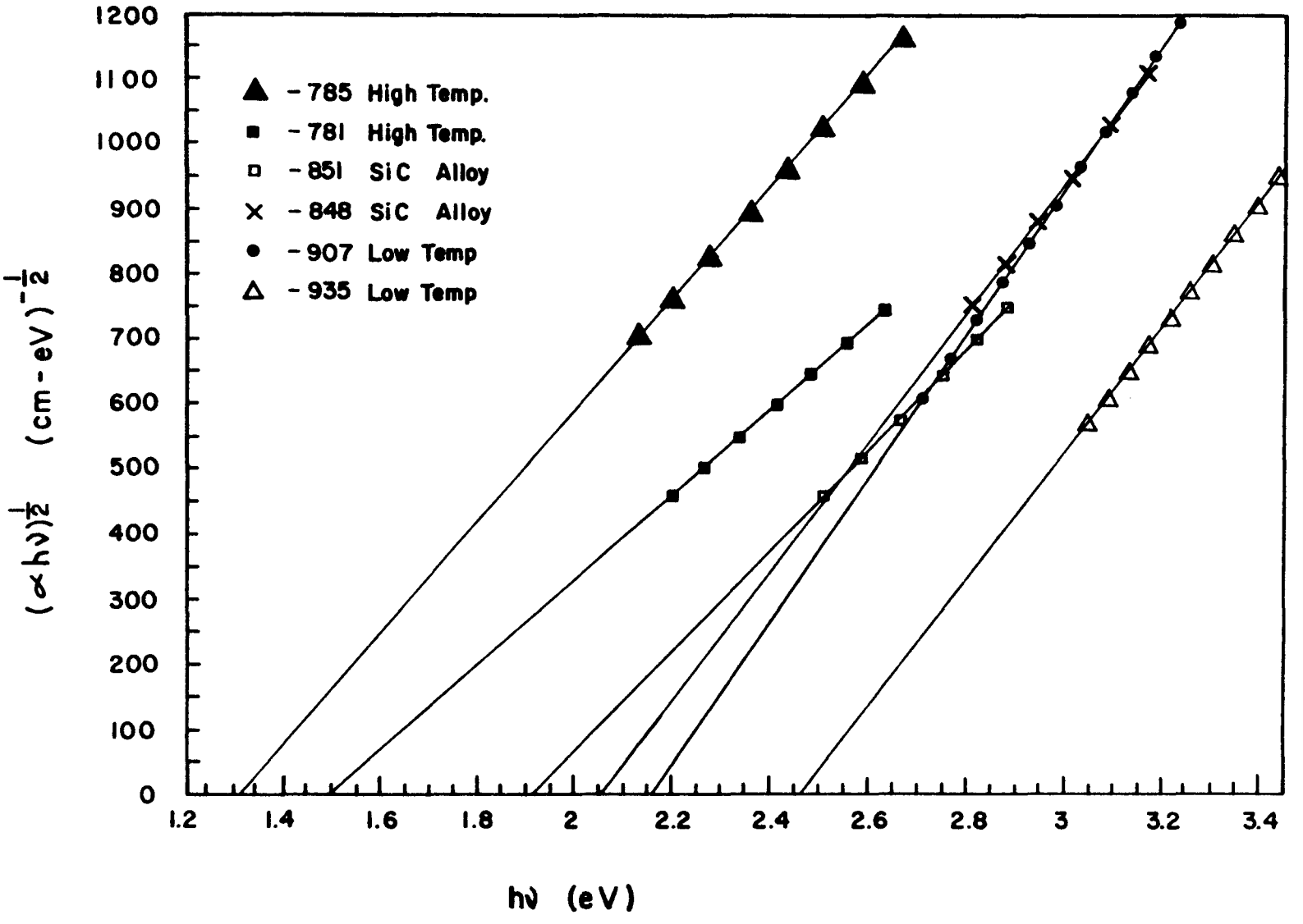

Fig. 2. Square root of the product of the absorption coefficient and the photon energy versus the photon energy for representative CVD p layers.

SERI/STR-211-2637

TABLE 2. Representative p layers as a function of temperature, pressure, ratio of initial diborane to silane concentration, and gas-phase residence time (R_t) in all CVD diagnostic Au/pin/ss devices illuminated by an ELH lamp at 100 mW/cm^2. For comparison, the V_{oc} of Au/in/ss Schottky diodes is 0.45-0.50 volts.

Sample	Silane	T_{sub}/T_{wall} (°C/°C)	Press. (Torr)	$\frac{[B_2H_6]_o}{[Silane]_o}$ (%)	R_t (Sec)	Time (Sec)	V_{oc} (Volts)
793	Monosilane	470[a]/400	20	0.7	13	45	0.36
791	Monosilane	470/400	2.2	0.7	1.5	60	0.40
774	Trisilane[b]	470/400	0.6	0.6	2.6	60	0.37
783	Trisilane	470/400	1.0	3.5	0.9	60	0.43
794	Monosilane	340/300	20	0.7	16	40	0.53
795	Monosilane	300/280	20	0.7	17	90	0.54
800	Monosilane	280/270	20	0.4	13	180	0.57
801	Monosilane	280/260	20	0.3	11	120	0.55
860	Trisilane	280/275	21	0.5	20	30	0.70
862	Trisilane	260/240	20	0.8	20	30	0.70
863	Trisilane	240/220	23	0.8	24	30	0.71
864	Trisilane	220/200	21	0.8	23	30	0.68
925	Disilane	200/180	2.3	1.5	3.2	120	0.62
866	Trisilane	200/180	20	0.8	25	60	0.71
868	Trisilane	200/180	10	0.8	20	90	0.71
869	Trisilane	200/220	6	0.8	7	120	0.72
902	Trisilane	200/180	2.5	1.5	3.5	120	0.70
873	Trisilane	200/180	2	0.8	2.4	120	0.72
870	Trisilane	200/180	1	0.8	1.1	150	0.66
867[c]	Trisilane	175/160	22	0.8	26	60	0.70

[a]This is the temperature of the stainless steel substrate holder. The actual substrate temperature is, in general, slightly cooler.

[b]The silane designated "trisilane" consists of a mixture of higher silanes, including disilane and tetrasilane, where trisilane is the major component.

[c]This run resulted in a poor device. It is possible that the p layer did not contact the i layer well.

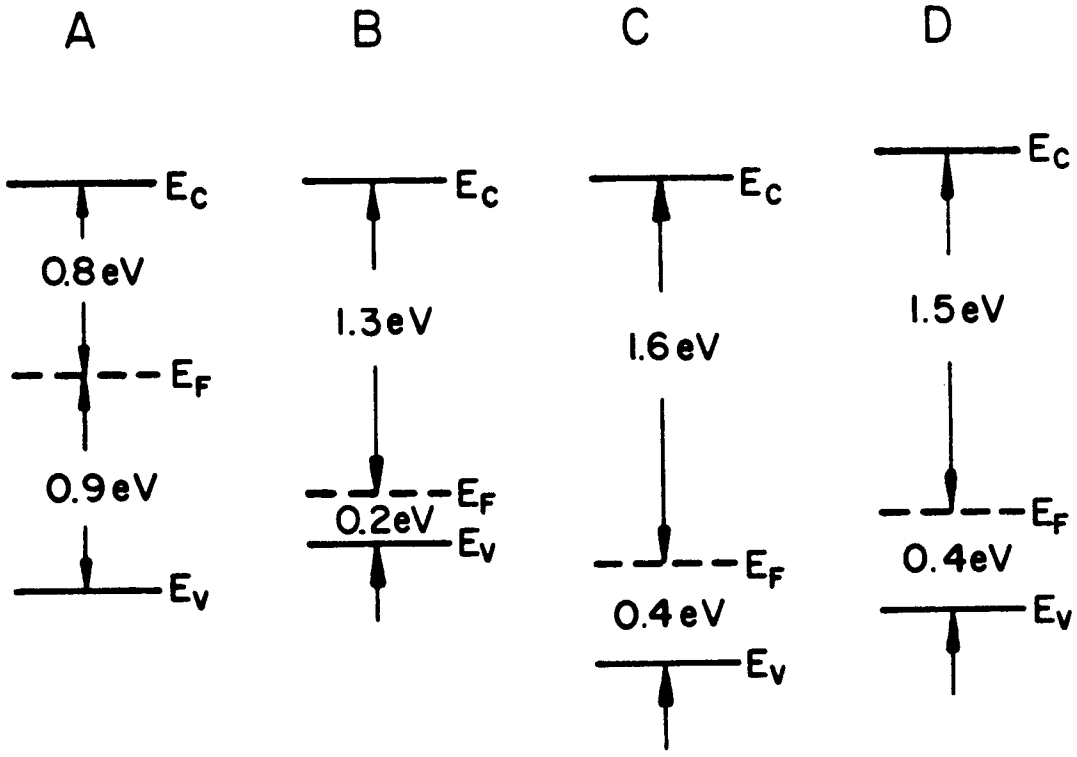

Fig. 3. Schematic diagram of relative positions of the band edges (E_V and E_C) and Fermi level (E_F) between a reference i layer (A), a high temperature CVD p layer (B), a low temperature CVD p layer (C), and a high temperature CVD silicon-carbon alloy p layer (D). This diagram was constructed assuming that the different V_{OC}'s observed in devices using these p layers arise mainly from the position of the Fermi level.

TABLE 3. Optical and electronic properties of CVD p layers. R_t is the gas-phase residence time. The dark contuctivity, σ_d, and the activation energy, E_a, are room temperature values; and the band gap, E_g, and the slope are measured in the usual way from $(\alpha h\nu)^{0.5}$ vs. $h\nu$.

Sample	Silane	T_{sub}/T_{wall} (°C/°C)	Press. (Torr)	$\frac{[B_2H_6]_o}{[Silane]_o}$ (%)	R_t (Sec)	σ_d $(\Omega\text{-cm})^{-1}$	E_a (eV)	E_g (eV)	Slope $(cm\text{-}eV)^{-0.5}$
785	Monosilane	470[a]/405	2.5	0.7	1.6	4x10-2		1.32	867
799	Monosilane	280/260	20	0.4	13	1-2x10-4			
781	Trisilane[b]	470/400	0.8	2.5	1.3	7×10^{-3}	0.20	1.50	659
782	Trisilane	470/400	0.9	3.7	0.9	1×10^{-2}			
850	Trisilane[c]	470/400	10	5.0	14	3×10^{-3}		1.43	660
851	Trisilane[d]	470/400	10	5.0	13	2×10^{-7}	0.37	1.91	763
849	Trisilane[e]	470/400	10	5.0	13	9×10^{-10}		1.94	787
848	Trisilane[f]	470/400	10	5.0	12	4×10^{-10}		2.06	996
927	Disilane	200/180	2.7	1.5	6.8			1.87[g]	840
928	Disilane	200/180	2.6	3.0	8.2	2×10^{-5}			
935	Disilane	200/180	50	0.04	610	9×10^{-10}		2.46[g]	968
907	Trisilane	200/180	2.4	1.9	6.9	5×10^{-7}	0.37	2.16[g]	1100

[a]This is the temperature of the stainless steel substrate holder. The actual substrate temperature is, in general, slightly cooler.

[b]The silane designated "trisilane" consists of a mixture of higher silanes, including disilane and tetrasilane, where trisilane is the major component.

[c-f]Acetylene is added to the higher silane mixture. The respective acetylene to silane ratios are: 0.13, 0.48, 0.66, and 1.1. Auger analysis of sample #851 shows Si:C:B = 48:45:7.

[g]These films are only about 0.2 microns thick. The band gap, as measured above, is thickness dependent. Thus, for comparison with the other films about 0.1-0.2 eV should be subtracted.

In the CVD of diborane and trisilane (containing some disilane and tetrasilane), the borane/silicon ratio in the film further decreased to 2-4 times the initial diborane/silane gas-phase ratio for deposition temperatures between 200 °C and 470 °C. For example, in the p layer of device #902 (see Table 2) the boron/silicon ratio in the p layer is about 4 percent according to Auger analysis. We argue below and present evidence for a high hydrogen content (can be greater than 25 atomic percent). Thus the above p layer should have about 3 atomic percent boron. An Arrhenius plot of the dark conductivity of a high temperature film prepared from trisilane and diborane (sample #781) is shown in Figure 4. The activation energy is 0.2 eV.

Referring to Table 2, one observes the trend of increasing Voc with increasing silane order and decreasing temperature. Thus for diborane/trisilane mixtures at 200-280 °C a Voc of 0.70 - 0.72 volts is obtained. For fixed boron concentration as the temperature decreases the band gap increases. This is undoubtedly a consequence of a high hydrogen concentration. At the low temperature range there is insufficient energy to break an unstressed silicon-hydrogen bond directly. Consequently it is expected that there are only two principal mechanisms for the loss of hydrogen from silicon-hydrogen bonds. The first occurs in both the gas phase and solid phase and is the hydrogen loss induced by the decomposition of diborane and the subsequent reactions. The second occurs only in the solid phase and is the hydrogen loss associated with reducing stress by bond rearrangement. However, at 200 °C there is not much energy available for bond rearrangement. These low temperature p layers are observed to buckle and peel from 7059 glass when more than about 0.2 to 0.3 microns are deposited, implying either poor film adhesion to glass and/or considerable stress within the film. Finally, a recent SIMS analysis of sample #935 indicated about 26 atomic percent hydrogen based upon comparison with a 17 atomic percent a-Si:H standard.

Referring to Table 3, one observes at 200 °C that the dark conductivity increases and the optical band gap decreases as the diborane/disilane ratio increases, or equivalently, as the concentration of boron in the film increases. The difference in the boron concentration would also explain why at comparable diborane/silane ratios the optical band gap is larger and the dark conductivity is smaller when starting with a larger order silane. Since at low diborane to disilane ratios it is possible to produce wide band gap material with disilane, it may be that with sufficient effort a Voc similar to the one obtained when using trisilane is possible for disilane.

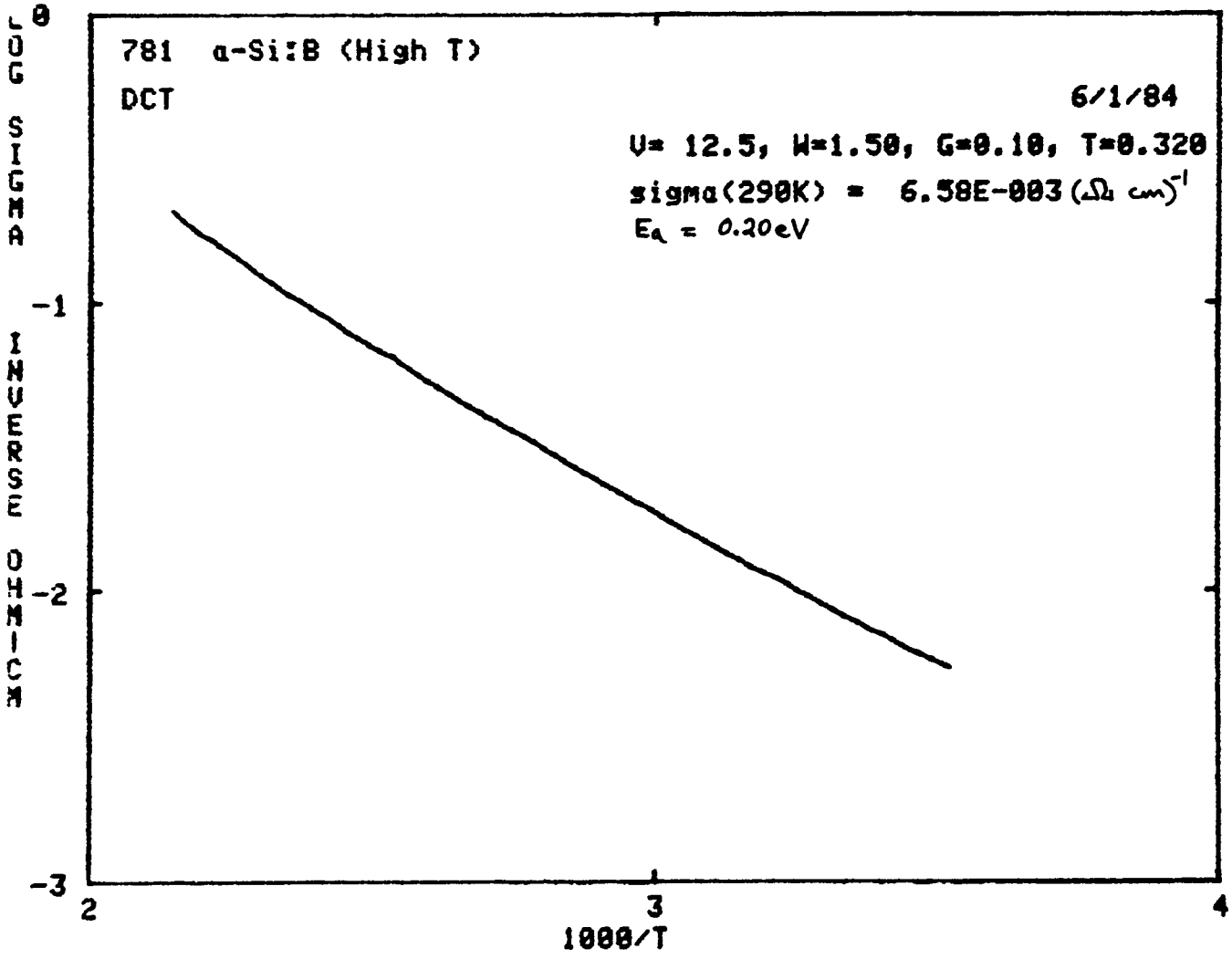

Fig. 4. Log dark conductivity versus inverse temperature for a boron doped a-Si:H film prepared at 470 °C from diborane and trisilane.

Figure 2 and Table 3 also show that the band gap may be increased at higher temperatures by adding acetylene to the silane-diborane mixture. At 470 °C, no deposition from acetylene on glass or c-silicon is obtained. Therefore, the carbon in the film arises from the interaction of acetylene with reactive silicon and boron-containing intermediates. From Table 3 it appears that the low temperature wide band gap p layer and the high temperature wide band gap silicon-carbon p layer can be deposited with very similar properties. For example, plots of the temperature dependence of the dark conductivity for samples #907 and #851 are practically identical (Figures 5 and 6). Thus both types of film should be useful in device application. However, to date at 440-470 °C and using acetylene/silane ratios from about 0.3 to 0.5, the Voc obtained using the carbon-containing p layer is between 0.45 and 0.56 volts. The largest Voc was obtained at the low acetylene/silane ratio.

Until more data are obtained, we must interpret these results cautiously. It may be that we have not found proper deposition parameters for use in devices. Alternatively, at the higher temperature used in silicon-carbon p layer, diffusion of boron into the i layer may be a problem. Another possibiliity may be contact problems between the p and i layer or a large recombination current in the p a-Si:H/i a-Si:H interface. The 10 to 80 percent smaller short-circuit current and generally smaller fill factor found in these devices tend to support the last two arguments.

On the other hand, as acetylene is added to the gas-phase mixture for low temperature p layers where diffusion of boron is not expected to be a problem the Voc again decreases. But adding sufficient acetylene to the silane-phosphine mixture at 470 °C to increase the band gap of the n layer by 0.2 to 0.3 eV and substituting this new n layer in CVD pin devices does not decrease the Voc. In fact, the built-in voltage appears to be slightly larger.* Assuming that the different Voc's stem to a significant degree from differences in the built-in voltage, then for a given band gap and activation energy these observations suggest a smaller work function in the n and p layers made from acetylene/trisilane mixtures. Thus, as acetylene is added to the higher silanes, the band gap of the resulting film increases at least in part by the shifting of the conduction band edge closer to the vacuum level (see Figure 3). If this is the case, then this type of wide band gap n layer has potential use in devices. Incidentally, a smaller acetylene/silane ratio is needed to produce an n layer of the same band gap as a p layer.

---

* At low temperatures Voc tends to the built-in voltage since the reverse dark saturation current is minimized. For a low temperature p a-Si:H/i-n a-Si:H device and for a low

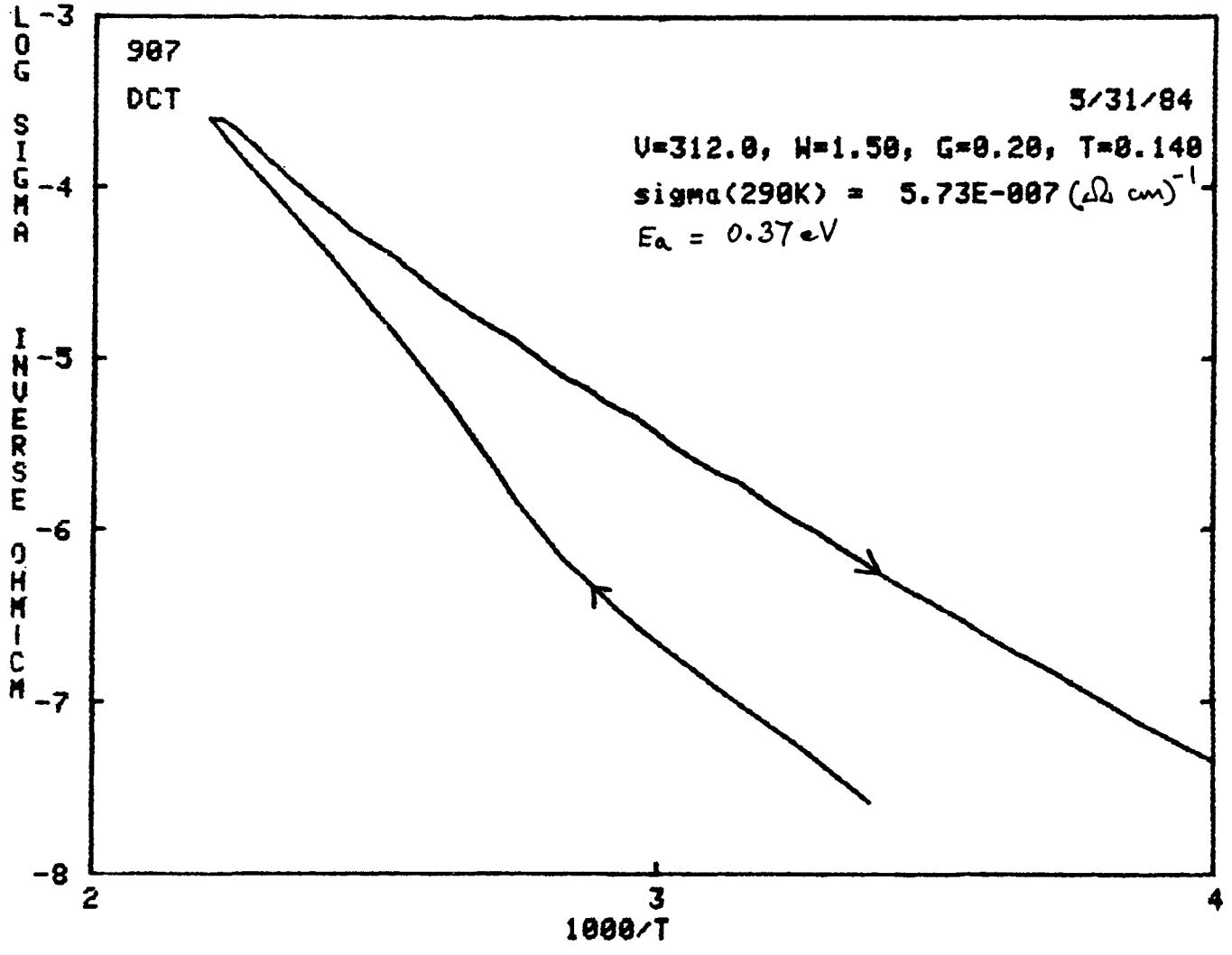

Fig. 5. Log dark conductivity versus inverse temperature for a wide gap boron doped a-Si:H film prepared at 200 °C from diborane and trisilane

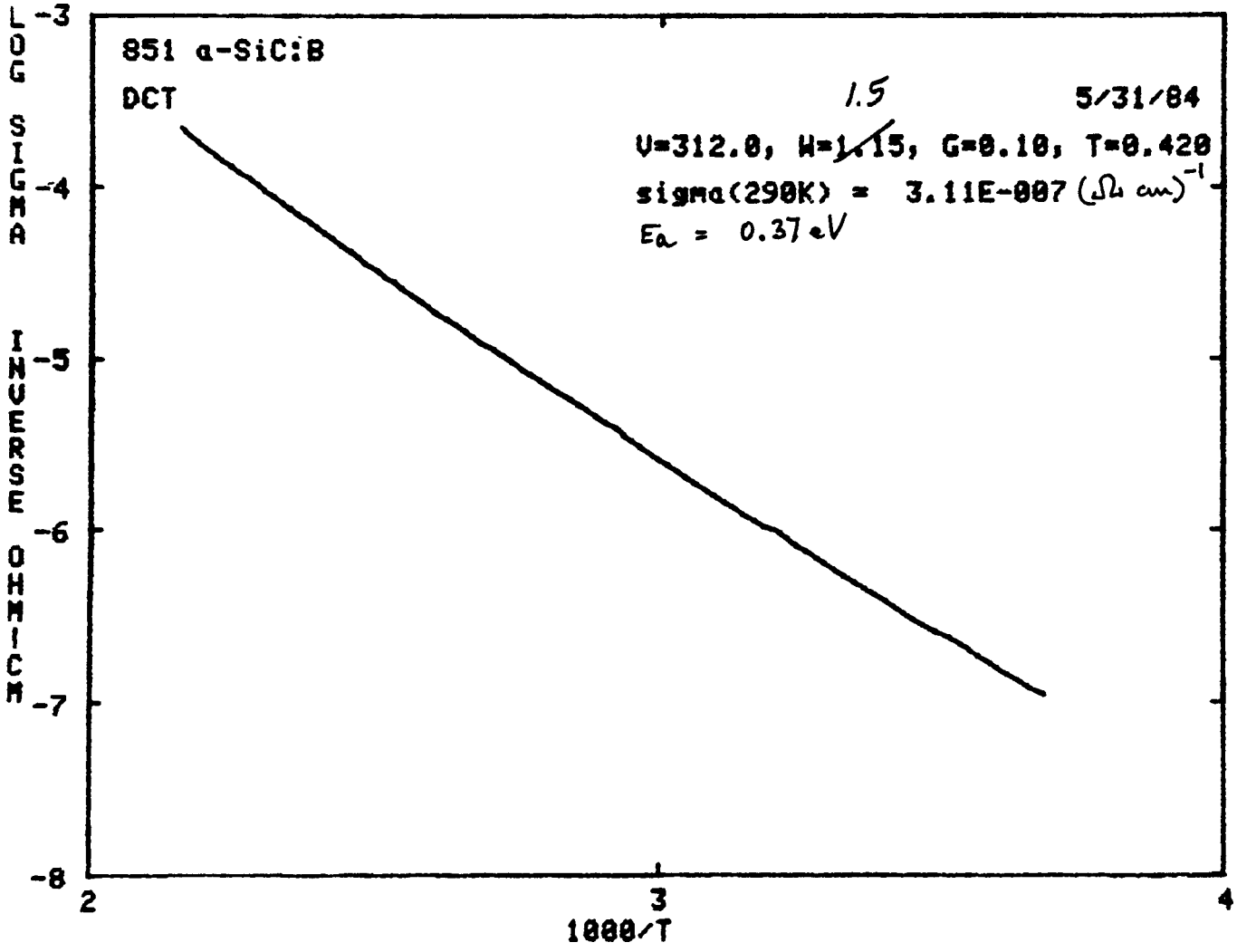

Fig. 6. Log dark conductivity versus inverse temperature for a wide gap boron doped a-Si,C:H film prepared at 470 °C from diborane, trisilane and acetylene

In conclusion, we have developed a CVD method, in the range of about 200 to 300 °C using higher order silanes, for depositing a wide band gap p layer without carbon. In an all CVD device, a typical Voc is between 0.70 and 0.72 volts and the best ITO/pin/ss devices have external solar conversion efficiency slightly greater than 3%.

2.1.2.3 N Layer Studies

N layers were made in the ususal way for both LPCVD and APCVD, namely by using mixtures of higher silanes and phosphine. In heavily doped films the room temperature dark conductivity is about 10^{-2} - 10^{-3} $ohm^{-1}cm^{-1}$ the activation energy is about 0.2 - 0.3 eV, and the optical band gap is slightly smaller than for undoped layers.

Wide band gap n layers were also investigated using mixtures of higher silanes and acetylene. Some properties of these films are reported in Table 4. When this type of n layer was used in p-i-n devices no loss in efficiency was observed. From low temperature measurements of Voc it appears that the built-in voltage may be slightly larger for devices with the wide band gap (1.8 - 1.9 eV) n layer. This suggests a smaller work function for the n layer (see section 2.1.2.2).

---

temperature p a-Si:H/i a-Si:H/n a-Si_xC_{1-x}:H device measured near the temperature of liquid nitrogen, the respective Voc'S were 0.99 V and 1.05 V.

Table 4. Properties of a-Si,C:H wide gap n layers produced using acetylene. In each case the total pressure was 20 Torr, the disilane and 10% PH_3 in Ar flow rates were 1.6 and 8.4 sccm, and Ts/Tw was 470 °C/400 °C.

Sample #	C_2H_2 (sccm)	Approx. growth rate (Å/S)	Approx. film thickness* (μm)	Eg (eV)	σd ($ohm^{-1}cm^{-1}$)	σp (AM1) ($ohm^{-1}cm^{-1}$)
965	0	1.7	0.41	1.61	2.7×10^{-3}	1.8×10^{-6}
963	0.54**	---	---	---	1.1×10^{-8}	1.7×10^{-8}
968	0.54**	1.0	0.35	1.82	9.6×10^{-10}	3.5×10^{-9}
967	0.67	0.6	0.21	2.04	1.2×10^{-9}	1.6×10^{-9}
966	1.9	0.7	0.25	2.6	1.1×10^{-9}	4.3×10^{-10}

* The film thickness was approximated by assuming an index of refraction of 3.6 and using interference fringes. Thus, except for #965 the thicknesses and growth rates may be underestimated by up to a factor of 2.

** Low end of flowmeter; setting may not be reproducible.

2.1.3 Atmospheric Pressure CVD (APCVD)

The deposition system is based on a rectangular 1 x 5 x 45 cm (ID) quartz tube which is heated from the underside by a nickel slab resting on a hot plate. The upper surface of the tube is insulated so that the resulting temperature gradient of 20 °C cm^{-1} ensures that particles nucleating in the gas phase are driven away from the substrate [6]. The higher silane gas mixture is mixed with a carrier gas (helium) in which the concentration of oxygen and water is reduced to about 0.1 ppm by means of a gettering furnace. The gas flow in the tube is laminar and exits through a graded diameter port to a decomposition furnace.

Very high growth rates for i layers produced in the atmospheric pressure flow system have been obtained, ranging from 14 to 87 Å s^{-1}. The hydrogen content of these a-Si:H films was determined quantitatively using the nuclear reaction technique. The results are shown in Table 5. The hydrogen content was found to be 16-17% depending on the partial pressure of the disilane and hence on the growth

rate; this value is slightly greater than the 14% hydrogen content of static CVD a-Si:H films.

Table 5. Hydrogen concentration in a-Si:H produced by atmospheric pressure flow CVD of higher silanes

Dep. Temp. (°C)	% Si_2H_6	Growth Rate (Å s^{-1})	H/(Si+H) (%)
435	4.1	43	16.9 ± 0.8
438	1.2	21	15.7 ± 0.8

The AM1 photoconductivity of undoped APCVD a-Si:H films lies in the range 10^{-7} to 10^{-6} ohm^{-1} cm^{-1}. This is disappointingly low. However, a study of light boron doping of the i layer greatly increased the ratio of the light conductivity to the dark conductivity. The deposition conditions and results are summarized in Table 6. For undoped films σp (AM1)/σd ranges from 1-5 x 10^3 , while for a diborane/disilane ratio of 1.75 x 10^{-4} this ratio increases to 4.3 x 10^4 . The energy gap for these films as determined by extrapolation of a $(\alpha E)^{1/2}$ versus E plot was 1.72 eV for 0.75 μm films (slope 800 $(eV\ cm)^{-1/2}$) and 1.77 eV for 0.54 μm films. Differences in the film thickness made it difficult to detect any change in energy gap due to the boron doping; if present, the gap shrinkage is 0.05 eV or less.

Table 6. Effect of light boron doping on atmospheric pressure CVD a-Si:H films.

Si_2H_6 (sccm)	10ppm B_2H_6 (sccm)	σd (ohm^{-1} cm^{-1})	σp (AM1) (ohm^{-1} cm^{-1})	$\sigma p/\sigma d$
4.5	0	1.6 x 10^{-10}	7.5 x 10^{-7}	4.7 x 10^3
2	5	1.2 x 10^{-10}	1.4 x 10^{-7}	1.3 x 10^3
2	20	8.5 x 10^{-11}	8.5 x 10^{-7}	1.0 x 10^4
2	30	4.8 x 10^{-10}	6.8 x 10^{-6}	1.4 x 10^4
2	35	1.4 x 10^{-10}	6.2 x 10^{-6}	4.3 x 10^4

deposition temperature 435 °C, He flow rate 350 or 375 sccm.

N-type films were produced by doping with phosphine. At high concentrations the dark conductivity is increased by a factor of 10^8 to $>10^{-2}$ $ohm^{-1}cm^{-1}$. Initial attempts to dope a-Si:H p type using triethylgallium as the dopant source were not successful due to powder formation [7]. The more thermally stable trimethylgallium remains to be tried.

Work concerning diffusion barriers was initiated. For example, 700 Å of TiO_2 was deposited by slow evaporation of Ti in an oxygen atmosphere onto tin oxide/7059 glass. The tin oxide had previously been electrolytically removed from the edges. The TiO_2 appeared bluish (oxygen deficient). The substrate was maintained at 435 °C for 15 minutes before deposition of a-Si:H. The a-Si:H film appeared reasonably specular. However, the tin oxide conductivity had increased to 800 ohms/square. We conclude that evaporated TiO_2 is not an adequate diffusion barrier between CVD a-Si:H and tin oxide.

2.1.4 Photo-CVD

A second generation mercury-sensitized photo-CVD deposition system was designed and constructed. It is shown schematically in Figure 7. The air space between the low pressure mercury lamp and the suprasil quartz window is flushed with nitrogen. The higher silanes enter the chamber after passing over a mercury reservoir held at 30-70 °C. The 253.7nm (4.89eV) light passing through the window is resonantly absorbed by mercury atoms present in the chamber. The excited mercury atoms exist in a long-lived triplet state; it is believed that they can abstract hydrogen from silanes, leading to a short lived intermediate HgH and silyl type radicals. The silyl radicals are precursors to a-Si:H film deposition. Direct decomposition of silane by vacuum-UV radiation (e.g. at 147nm) is also possible and results in SiH_2+ 2H (yield 0.83) or SiH_3 + H (yield 0.17), while silane decomposition via multiphoton absorption from a CO_2 laser yields SiH_2 + H_2. However, only the mercury-sensitized decomposition scheme has been pursued under this contract.

With the intention of reducing a-Si:H deposition on the window, a flushing gas (helium) was introduced into the chamber just under the window to reduce the silane partial pressure in that region. However, for the system geometry of Figure 7 we were not successful in suppressing window deposition by this means.

Initial runs were made using monosilane as the source gas. The first few runs resulted in visible deposition on the window but no deposition at all on the substrates. The metal baffles were removed and the substrates were then placed on a cylindrical aluminum block to bring them closer to the window. In this way an a-Si:H film was produced but its thickness was less than 100 Å. Next disilane was substituted for silane and somewhat thicker films were obtained (150-200Å). A σ_p (AM1)/σ_d ratio of 10^4 was obtained for run G6031. These results are summarized in Table 7. With the aluminum block removed , the flow rate of He had to be greatly increased to compensate for the increased volume of the chamber, and possibly to confine the Si_2H_6/Hg to the vicinity of the substrate.

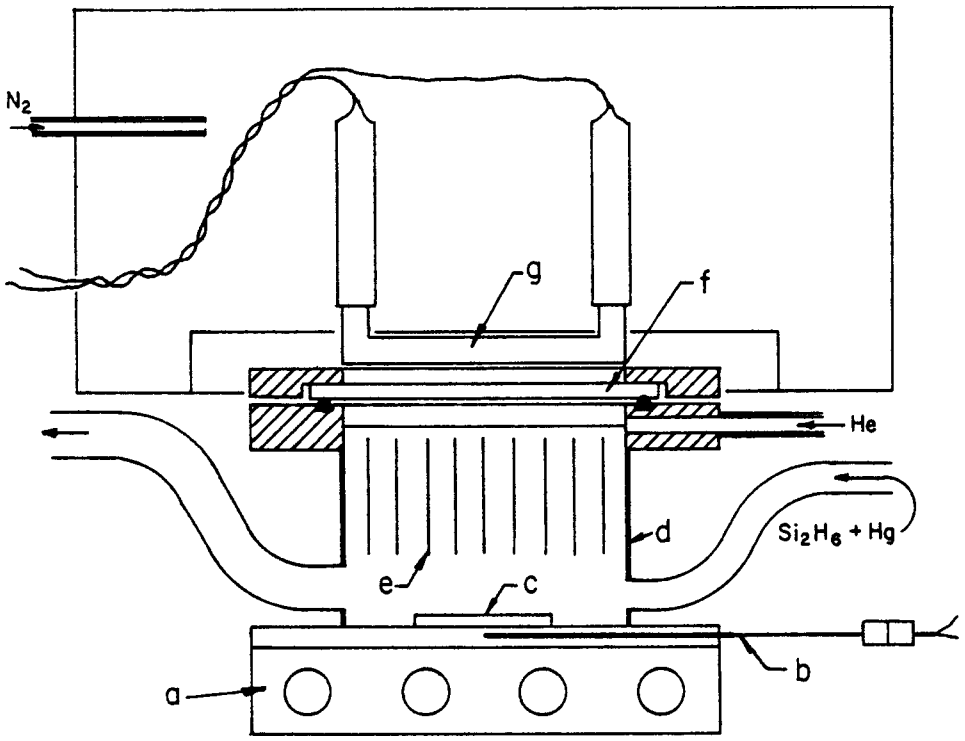

a. Aluminum Heater Block
b. Thermocouple
c. Substrate
d. Stainless Steel Chamber
e. Baffles
f. Suprasil Quartz Window
g. Low Pressure Mercury Lamp

Fig. 7. Photo-CVD system (mercury sensitized)

TABLE 7. Deposition conditions and properties of photo-CVD a-Si:H Layers

Run #	Window -sub. (cm)	Window Grease	Temp. Hg (°C)	Temp. Sub (°C)	Dep. Time (min)	Press. (Torr)	Flow Rates (sccm) He	SiH_4	Si_2H_6	Film Thickness (Å)	σ_d $(ohm\text{-}cm)^{-1}$	σ_p (AM1) $(ohm\text{-}cm)^{-1}$
G6009	5.9	none	30	220	40	20	46	6	-	on window only	-	-
G6015	1.6	none	55	270	60	20	10	10	-	<100	1.8E-10	1.6E-8
G6025	1.6	none	24	270	30	10	5	-	5	150	5.9E-9	4.7E-6
G6031	1.6	none	24	280	30	2	5	-	5	200	1.6E-9	1.6E-5
G6035	5.9	none	24	250	30	1.5	2	-	5	<100	-	-
G6037	5.9	none	70	250	30	10	180	-	20	-	3.6E-9	4.6E-7
G6045	5.9	none	70	250	60	5	180	-	8	600	6.1E-9	1.1E-5
G6056	5.9	type BR	70	250	30	5	180	-	5	-	3.3E-3*	9.9E-3
G6088	5.9	type BR	70	240	60	5	180	-	8	764	2.2E-10	7.6E-7
G6092	5.9	type F/F	70	240	180	5	180	8	-	2260	1.3E-9	1.9E-5
G6096A	5.9	type BR	70	240	180	5	180	-	8	2150	2.8E-9	6.0E-6
G6096B**	5.9	type BR	70	240	180	5	180	-	8	760	9.3E-10	2.7E-6

Hg carried by He,not the silane
* doped using 1 sccm 10% PH_3 in Ar
** fine mesh used under window

SERI/STR-211-2637

Further attempts to prevent a-Si:H deposition on the quartz window were made by freshly coating the inside surface of the window with various low vapor pressure oils prior to each run, as had been mentioned by workers at the Tokyo Institute of Technology [8]. Of the four types of oils and grease that were tried only one (type BR) worked satisfactorily, yielding no deposition on the window and a film on the substrate. Using this grease a-Si:H films of about 2200Å in thickness could be grown in 3 hours, corresponding to an average growth rate of 0.2Å s^{-1} .

The optical band gap of photo-CVD a-Si:H i layers, as determined by the conventional $(\alpha E)^{1/2}$ versus E plot, was found to be 1.88 eV and 1.84 eV for 2200Å films prepared from silane (run G6092) and disilane (run G6096A) respectively.

A phosphorus-doped n layer (run G6056) was grown using a disilane flow rate of 5sccm plus 1sccm of 10% phosphine in argon. A dark conductivity of 3.3 X 10^{-3} ohm^{-1} cm^{-1} and an AM1 photoconductivity of 9.9 X 10^{-3} ohm^{-1} cm^{-1} were achieved.

The dark conductivity and photoconductivity of photo-CVD run G6062 (an i layer) were measured in a co-planar configuration as a function of temperature. The room temperature dark conductivity was 1.0 X 10^{-10} ohm^{-1} cm^{-1} . The thermal activation energy, as calculated directly from $\sigma(T) = \sigma_o \exp(-\Delta E/kt)$ assuming σ_o = 200 ohm^{-1} cm^{-1} , was 0.71 eV at room temperature, or as determined from the slope of an Arrhenius plot, 0.65 eV at room temperature and 0.88 eV near 200°C. The Arrhenius plot is shown in Figure 8.

The temperature dependence of the photoconductivity, as measured with a photon flux of 8 X 10^{14} photons cm^{-2} s^{-1} at 600nm, is shown in Figure 9. It is interesting to note that the photoconductivity exhibited a low temperature peak and thermal quenching ("Delahoy dip" or "Vanier valley") for 1000/T between 8 and 5 (125K to 200K). These features are usually observed in undoped glow discharge films [9] (and never in thermal CVD films [1]) suggesting that photo-CVD a-Si:H possesses a gap state distribution similar to glow discharge a-Si:H. This implies the existence of two types of states in the gap (states 1 and 2) one of which is the dangling bond (states 2). It is tempting to speculate that unless atomic hydrogen is present during the deposition of a-Si:H this structure in photoconductivity does not occur. The atomic hydrogen may a) reduce the dangling bond density to allow observation of thermal quenching, and/or b) actually introduce states 1 having a low electron capture cross section [9]. The cause of the small hump in photoconductiviy that appears over a narrow temperature region near 1000/T = 4 is unknown, but it could result from surface

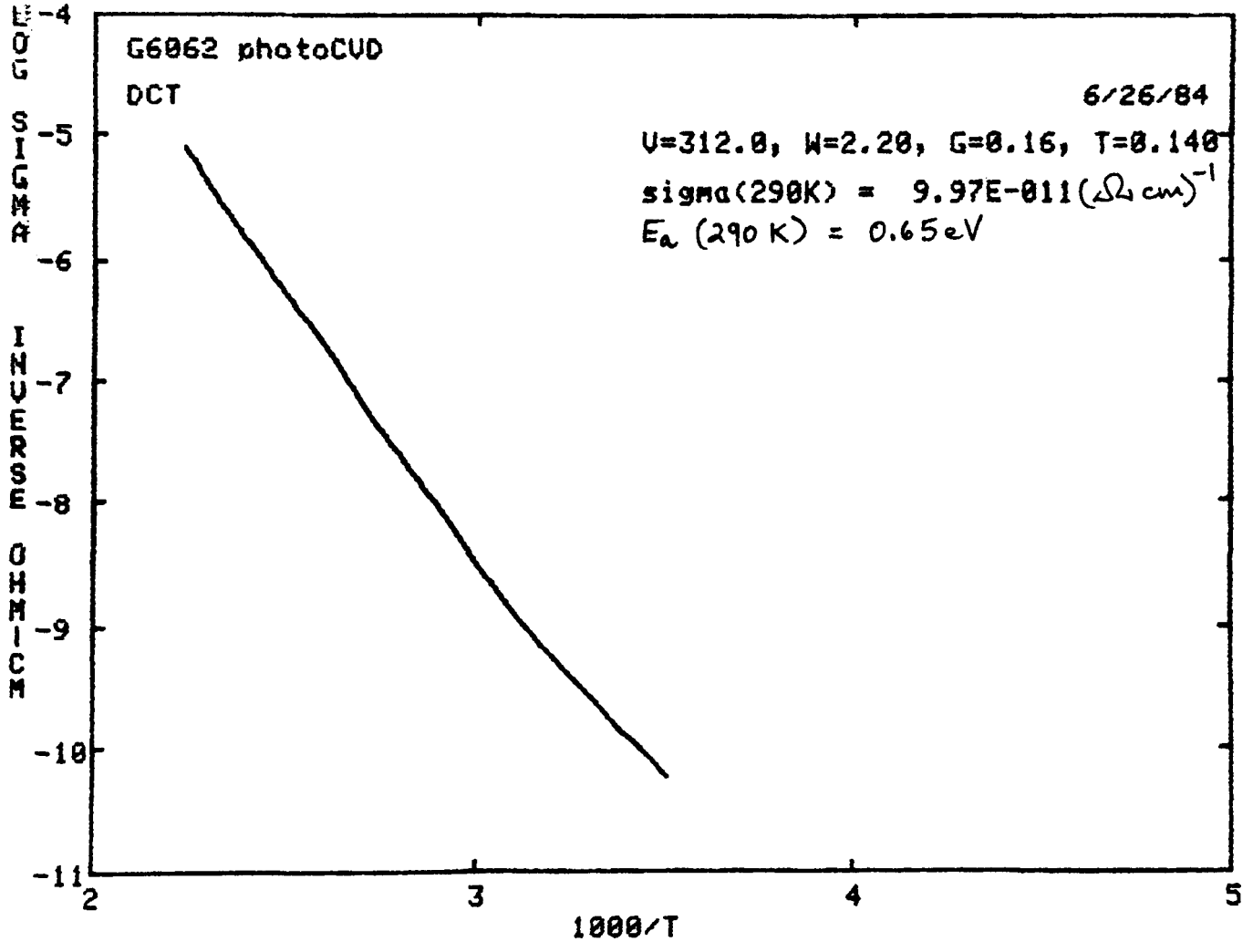

Fig. 8. Arrhenius plot of the dark conductivity of an undoped a-Si:H film prepared by photo-CVD

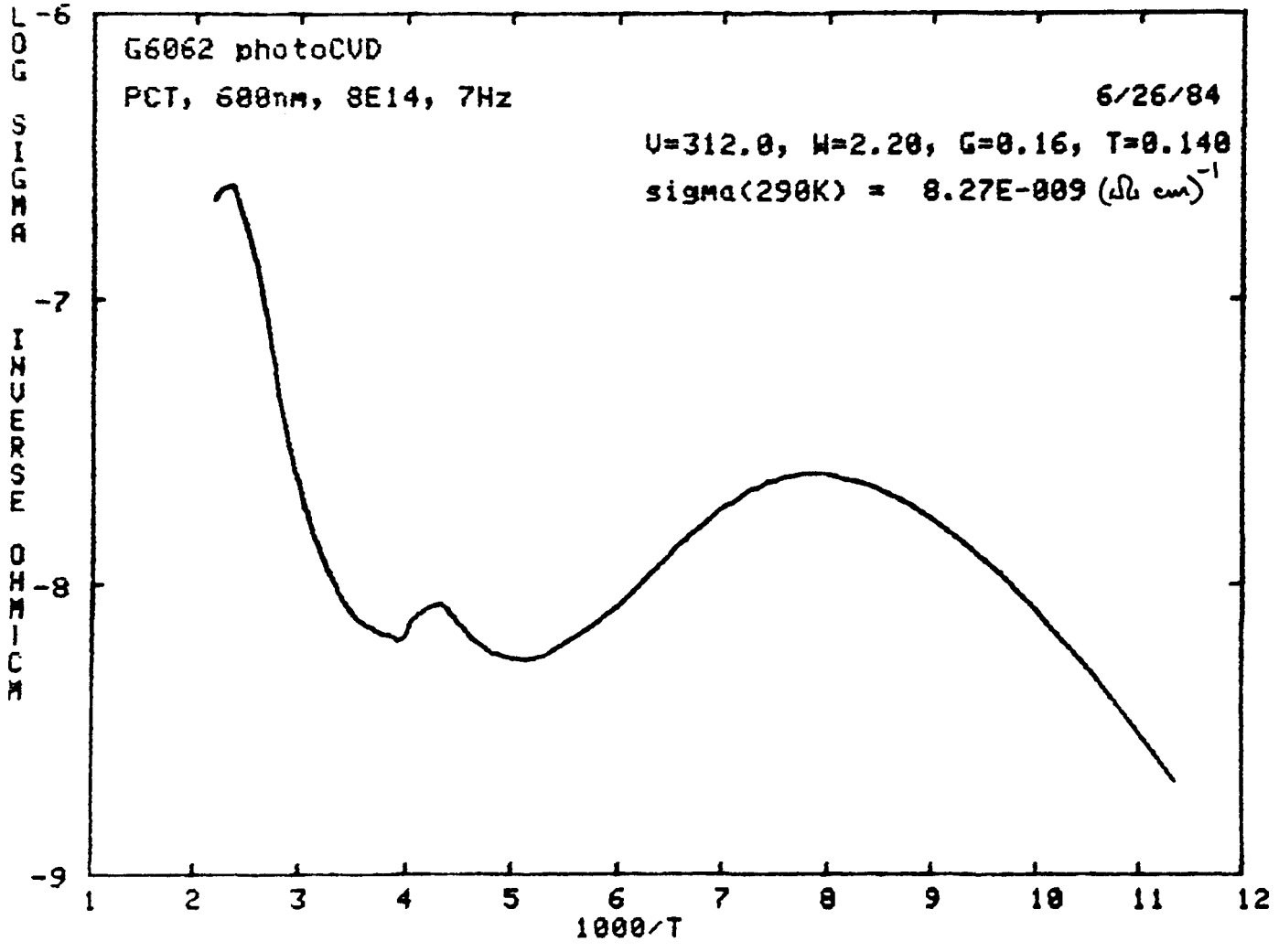

Figure 9: Photoconductivity versus inverse temperature for a photoCVD a-Si:H i layer. Thermal quenching is observed for $5 < 1000/T < 8$.

states or reconstruction of a specific defect. A similar hump is often seen in glow discharge films. The elucidation of this effect might well prove to be informative.

Despite improvements in deposition rate made by flushing the air space between the mercury lamp and the window with nitrogen, and by coating the inside of the window with a low vapor pressure grease, the low deposition rate (0.2Å s^{-1}) remains a major problem. Increasing the voltage applied applied to the lamp transformer by 10%, or doubling the current to the lamp by using two (current limiting) transformers in parallel did not result in noticeably thicker films. This was possibly due to broadening of the 2537Å line, since proportionately greater total UV outputs from the lamp were measured. The temperature of low pressure mercury lamps is known to strongly affect the emission intensity of resonance radiation, although we have not yet attempted to exploit this fact. A more intense source of 2537Å resonance radiation is certainly part of the solution to the low deposition rate problem and this possibility will be explored. Also, there is no reason to think that the type of grease currently used for the window coating is optimal. Indeed, we are now experimenting both with methods of coating application eg. dissolving the grease in a solvent (freon), and with other fluorinated materials as window coatings.

2.2 TASK 2: COMPARATIVE EVALUATION OF VARIOUS CVD TECHNIQUES

Based on results reported in section 2.3 (Device Fabrication and Analysis) we can definitively state that LPCVD is capable of producing higher efficiency devices than static CVD (in both Schottky and p-i-n configurations). These results confirm the reasoning outlined in section 1.1. Deposition Methods. The present data do not distinguish between LPCVD and APCVD, both having attained 1.2% efficiency for Schottky devices (see Table 8). The highest efficiency devices, however, have been prepared by photo-CVD, and progress in this area has been rapid. For example, a single stack device efficiency of 4.4% was obtained by photo-CVD in under six months of device work, compared to 3.1% by LPCVD for over one year of research.

The inferior photovoltaic performance of LPCVD cells compared to photo-CVD cells cannot be ascribed to common impurities such as carbon, oxygen, nitrogen and chlorine, for SIMS analyses of these films show significantly lower concentrations of these elements in LPCVD films than in photo-CVD films, and except for chlorine, the LPCVD concentrations are lower even than for high quality glow discharge a-Si:H films (see Figures 10 and 11, and Table 9). The concentration of atmospheric impurities (O and N) appears roughly comparable for photo-CVD and glow discharge films, although the photo-CVD films appear to have a fairly high carbon content (3×10^{19} cm^{-3}). The origin of this carbon may be the window coating material. It is of interest to note that mercury could not be detected in the photo-CVD films by SIMS at a sensitivity limit of about 1×10^{18} cm^{-3}. The sharpness of the p-i interface for photo-CVD devices having the structure glass/SnO_2/p-i-n/ metal was also found to be comparable to that of high efficiency p-i-n devices prepared by glow discharge.

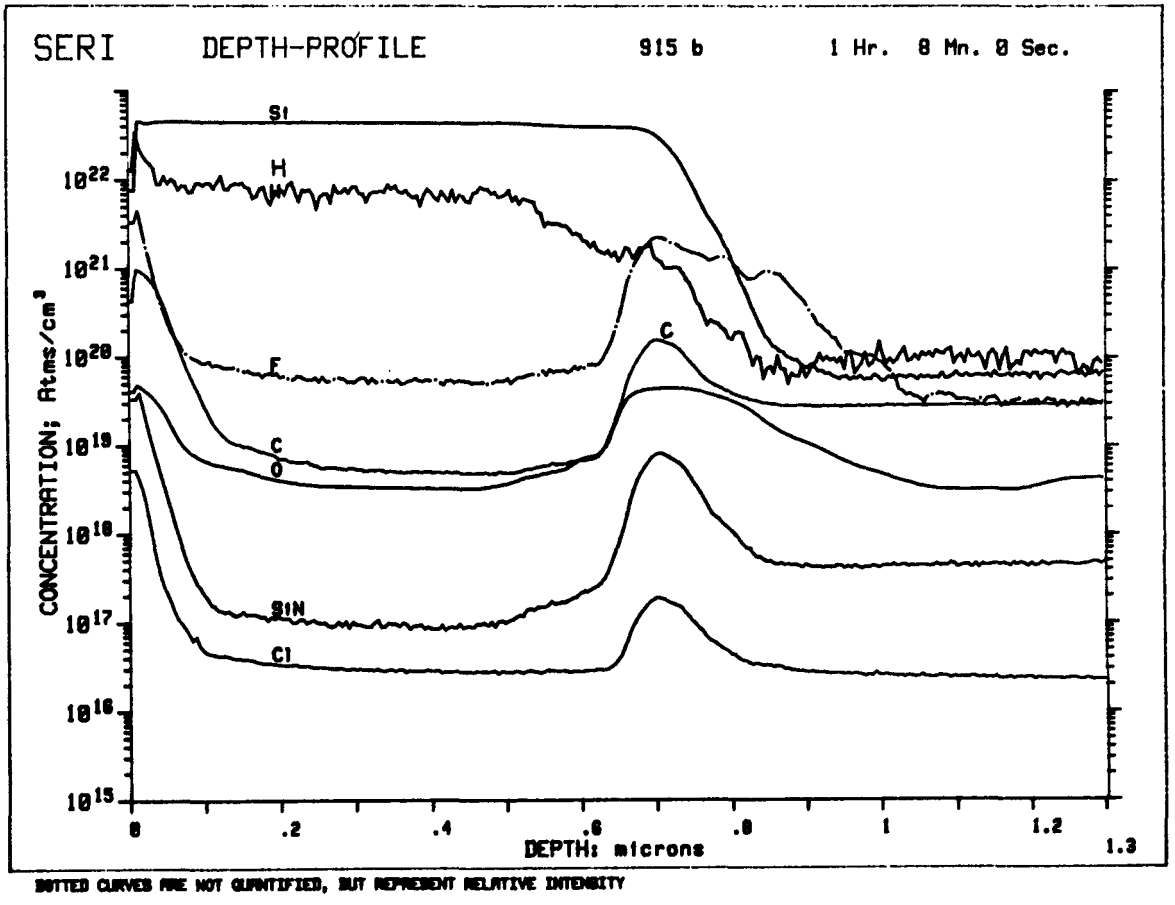

Fig. 10. SIMS depth profile of a p-i-n device deposited by LPCVD

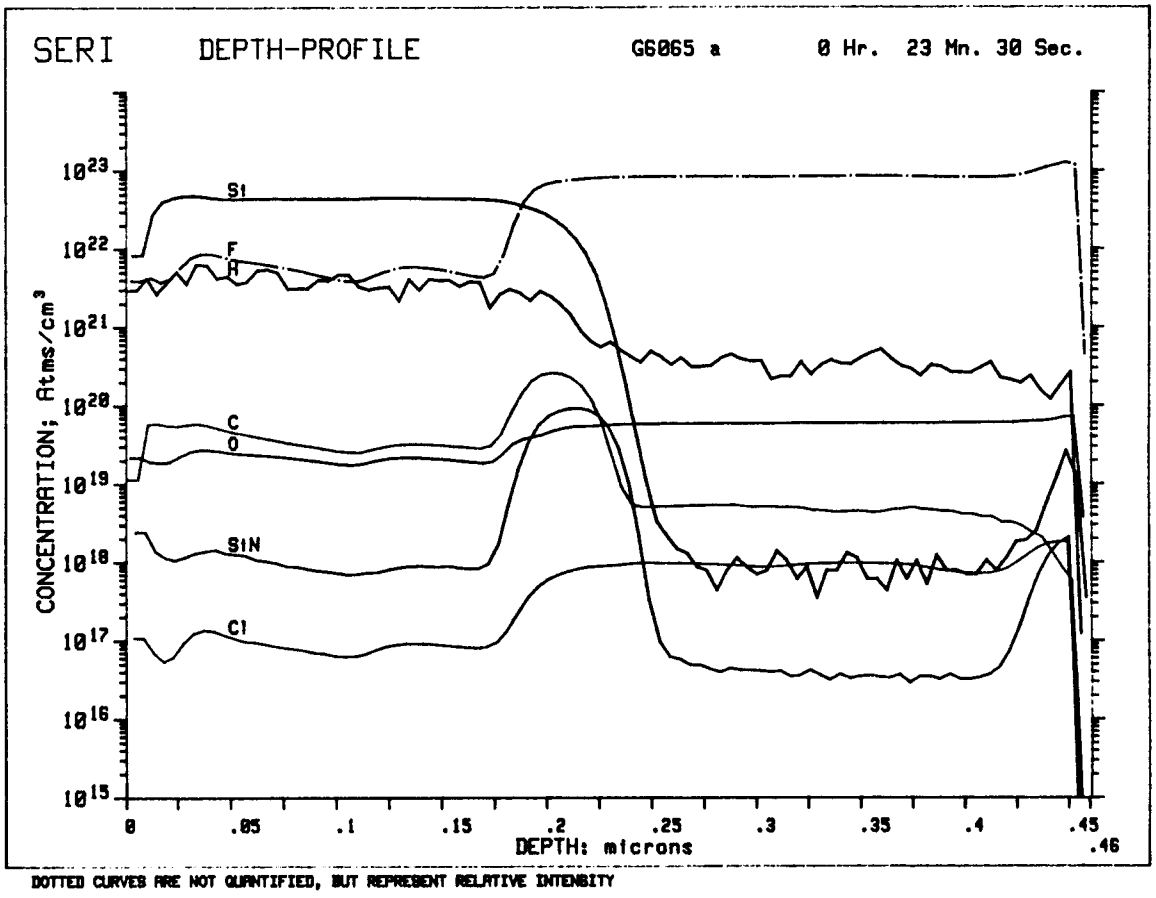

Fig. 11. SIMS depth profile of a p-i-n device deposited by mercury-sensitized photo-CVD

Table 8. Comparison of CVD techniques based on photovoltaic parameters of the most efficient (single stack) device prepared by each technique as of 8/31/84.

		Static CVD	LPCVD	APCVD	Photo-CVD
Voc (V)	Schottky	0.48	0.49	0.52	0.45
	PIN	0.62	0.66	-	0.66
Jsc ($mAcm^{-2}$)	Schottky	3.7	4.9	5.5	7.4*
	PIN	5.9	10.0	-	10.1
FF	Schottky	0.42	0.49	0.41	0.60
	PIN	0.37	0.46	-	0.66
Eff(%)	Schottky	0.75	1.2	1.2	2.0
	PIN	1.4	3.1	-	4.4

* In contrast to the other Schottky diodes, the photo-CVD Schottky diodes are not illuminated through a gold contact but through a tin oxide layer.

Table 9. SIMS analysis of a-Si:H films prepared at Chronar by rf glow discharge, LPCVD, and mercury-sensitized photo-CVD.

Species	Concentration (atoms cm^{-3})		
	glow discharge*	LPCVD	photo-CVD
H**	16%	16%	10% (?)
C	7E18	5E18	3E19
O	2E19	3E18	2E19
N	5E17	1E17	1E18
Cl	1E16	3E16	1E17
Hg	-	-	undetectable
transition elements	undetectable	undetectable	undetectable
	ratio of peak in p layer to background in i layer		
B	1E4	-	2E4
Sn	2E4	-	1E4

substrates were glass/SnO_2 for glow discharge and photo-CVD films, and stainless steel for LPCVD films.
* films prepared in the D system operated under subcontract ZB-3-03056-1
** SIMS data normalized to [H] obtained for LPCVD films by the nuclear reaction technique

Whether the diffusion of impurities (such as Cr or Fe) from the steel substrate into the a-Si:H film might partially

account for the inferior performance of LPCVD devices is not clear. We have not observed improved performance in stainless steel/n-i-p/ITO devices prepared by LPCVD where the n layer is 2000Å thick, rather than the usual 500Å, where the extra 1500Å (n type) a-Si:H can be interpreted as a "diffusion barrier" between the substrate and the i layer. After much work, LPCVD device efficiencies never rose above 3.1%, and it is our belief that substrate-related impurities are not the limiting factor.

We should like to advance the hypothesis that a-Si:H prepared by thermal CVD of higher silanes suffers a loss of hydrogen from crucial sites (due to annealing of the already deposited film at the high deposition temperature) leaving behind an unavoidable minimum density of defects (probably dangling bonds). For example, if only 1% of the bonded hydrogen atoms are evolved due to annealing, and if a dangling bond is left behind at only 0.2% of these sites, then approximately 1×10^{17} dangling bonds per cm^3 are created. If this is true, CVD a-Si:H possesses a fundamental limitation in its electronic properties. Another factor that may contribute to an unacceptably high dangling bond density is the probable lack of atomic hydrogen during growth. Among other things, the presence of atomic hydrogen would probably improve surface mobility.

2.3 TASK 3: DEVICE FABRICATION AND ANALYSIS

2.3.1 Low Pressure CVD Devices

Optimization of i-layer deposition conditions in the LPCVD system was carried out using a Schottky barrier device configuration (Au/i-n+/ss) which experience had shown to work well. No AR coating was used. A study was made of LPCVD Schottky diode characteristics as a function of flow rate at a given temperature and pressure. The results are shown in Table 10.

Table 10. Effect of disilane flow rate on the performance of Schottky diodes prepared by LPCVD.

Sample #	Flow rate (arb. units)	Thickness (μm)	Voc (V)	Jsc ($mAcm^{-2}$)	FF	Eff. (%)
760	10	0.5	0.41	2.9	0.51	0.61
762	15	0.6	0.45	3.75	0.52	0.87
763	15	0.6	0.46	4.35	0.52	1.05
764	20	0.7	0.45	4.1	0.53	0.99
765	30	0.9	0.49	4.9	0.49	1.18
766	40	0.8	0.49	4.3	0.48	1.00

T sub = 470°C, T wall = 400°C, pressure = 15 Torr, i-layer deposition time = 10 mins, Au thickness = 100 Å, no AR coating.

It is interesting to note that the efficiency did not peak at an i-layer thickness of 0.5μm as it did for static depositions. In fact the highest efficiency was obtained at 0.9 μm, with other experiments showing good results at 1.6 μm. It seems likely that a superior electron $\mu\tau$ product is obtained in the flow CVD method compared to that obtained by static CVD. We also note from Table 10 that the best Schottky diode occured at the flow rate which gave the highest growth rate at the substrate. A further observation is that Voc increases with increasing i-layer thickness. The spectral response of these LPCVD Schottky cells indicate classical a-Si:H behavior with hole transport limiting the carrier collection. The latter conclusion is deduced from the variation of the QE(OV)/QE(-0.5V) curve with wavelength.

It has occurred to us that if LPCVD a-Si:H possesses a density of dangling bonds higher than is desired, then post-deposition hydrogenation (i.e. exposure to atomic H) might serve to improve the material. The results of an initial photo-hydrogenation study are shown in Table 11.

Table 11. Photo-hydrogenation study; performance of control and treated Au/i-n^+/ss Schottky devices.

Cell	a-Si:H treatment prior to metallization				Voc	Jsc	FF	Eff
	325 °C	He	H_2	UV light*	(V)	($mAcm^{-2}$)		(%)
978A	-	-	-	-	0.39	4.0	0.52	0.81
978B	✓	✓	-	-	0.39	4.1	0.50	0.79
978C	✓	✓	-	✓	0.40	3.7	0.51	0.76
978D	✓	-	✓	✓	0.49	3.5	0.51	0.87

*without mercury sensitization.
flow rates: H_2 5 sccm, He 180 sccm
pressure: 5 Torr
time: 20 min.

No mercury was present in the chamber. The results seem to suggest that Voc can be increased by exposure of the LPCVD a-Si:H to molecular hydrogen and UV light prior to metallization. This is surprising since hydrogen is essentially transparent down to 1100 Å and atomic hydrogen would not be expected to be produced. Since it is known that Hg sensitization definitely produces atomic H (the Hg 6 $^3P_1$ excitation energy is 4.88 eV while the heat of dissociation of H_2 is 4.45 eV) this will next be tried.

We now turn our attention to p-i-n devices. Because poor Voc's had been observed in p-i-n devices made by CVD while reasonable (and similar) Voc's were observed in metal/i-n^+/ss Schottky diodes made by CVD or glow discharge, we felt that the CVD p layer was in need of considerable improvement. Knowing that diborane catalyzes the decomposition of silanes we decided to investigate silane, disilane, and trisilane for deposition of the p layer. This study is described in detail in section 2.1.2.2. By lowering the p layer deposition temperature from 470 °C to 200 °C, and the pressure from 23 Torr to 2 Torr, an open-circuit voltage of 723 mV was obtained in a Au/p-i-n/ss device with no powder by-product during deposition of the p layer. Short-circuit current densities of up to 7 mA cm^{-2} were attained. Surprisingly, both Voc and the effective transmission of the p layer as measured by Jsc were quite insensitive to the deposition pressure (1-23 Torr), and to the flow rates of the higher silane mixture (10-35 sccm) and diborane mixture (15-34 sccm). Some powder was formed on the cold walls for pressures >5 Torr. The open-circuit voltage is , however, very sensitive to the amount of trisilane in the higher silane mixture.

An annealing study was performed to try to understand the superior performance of the low temperature p layer (see Table 12). The decrease in cell performance after annealing of the p layer could stem from a loss of hydrogen from the low temperature p layer, diffusion of boron into the i layer, or loss of hydrogen from the i layer. The possible loss of hydrogen from the p layer would reduce its band gap, thereby reducing Jsc and possibly Voc. This could be tested by measuring the energy gap and activation energy of low temperature p layers before and after annealing.

Table 12. Comparison with standard cells of diagnostic Au/p-i-n/ss solar cells formed after annealing the a-Si:H layers at 470°C for 5 minutes. The n and i layers were deposited at 470°C while the p layer was deposited at 200°C.

Sample	Voc (V)	Jsc (mA cm^{-2})	FF	Eff (%)
Standard	0.70	5.1	0.51	1.8
Annealed	0.60	3.7	0.50	1.1

Another area of investigation has been the influence of different silane mixtures on the LPCVD i-layer. We observed that increasing the amount of trisilane in the predominantly disilane mixture tends to decrease the fill factor by up to 13%. On the other hand we have found that some improvement in the fill factor is possible through the addition of monosilane to the higher silane mixture for deposition of the i layer. Data for 14 runs are shown in Figure 12. The variations in fill factor are almost certainly representative of the changing silane mixture and not due to changing thickness since Jsc was fairly constant. By this technique fill factors up to 0.56 have been achieved.

We have also found that the optimum flow rate is considerably different for pure disilane and mixtures which include a significant trisilane concentration. For the former case lower flow rates are needed and smaller growth rates are obtained (see section 2.1.2.1). For the Japanese gas (0.7% trisilane, see section 2.1.1) monosilane dilution of the disilane for the i layer was not beneficial. According to Au/pin/ss diagnostic devices the i layer formed from the Japanese gas tended to be somewhat inferior as measured by Jsc and FF. The poor Voc (generally 0.5V) probably indicates a poor quality p layer. Recall that we previously observed that Voc increased with increasing fractional amount of trisilane. The best device (sample #946) obtained with the Mitsui Toatsu disilane had the following characteristics:

Voc	Jsc	FF	Eff
0.57 V	5.1mAcm^{-2}	0.49	1.4%

which is 40% less efficient than what we have obtained using Chronar SED gas for the same configuration (Au/p-i-n/ss). A complicating factor, however, was the observation of higher open circuit voltages after cleaning of the deposition chamber. The cleaning was performed shortly after the study involving the Mitsui Toatsu disilane.

The effect of i-layer thickness on Au/p-i-n/ss diagnostic solar cells is given in Table 13. Note that Jsc increases with increasing thickness, suggesting that there is some current collection throughout the i-layer. The decreasing fill factor is consistent with the model in which the fill factor is determined by the ratio Lco/L i.e. the ratio of collection length ("film quality") to the film thickness.

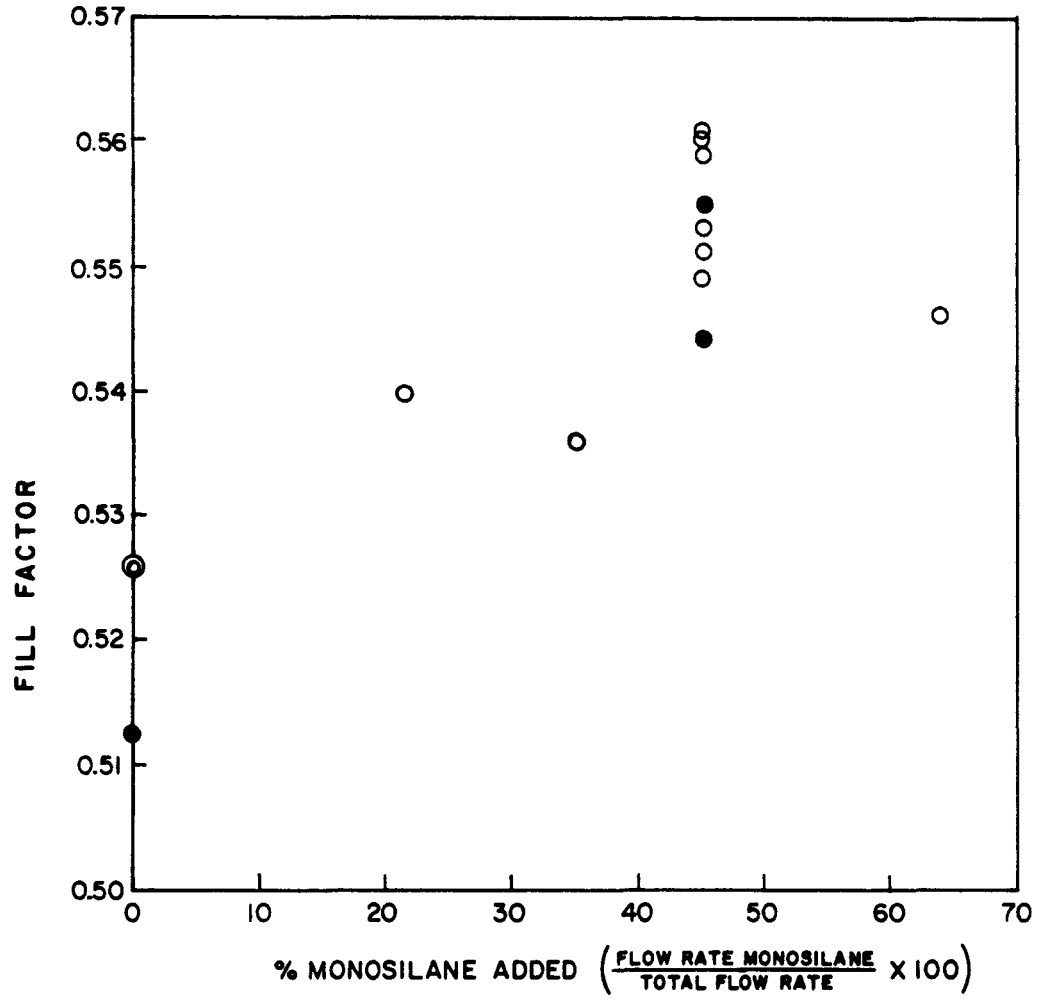

Figure 12: Variation of fill factor as a function of the silane mixture; the higher silanes were diluted by the addition of monosilane. Solid circles (●) denote depositions performed with an almost empty cylinder of higher silanes, corresponding to an increase in the fraction of the less volatile silanes (mainly trisilane).

Table 13. The effect of i-layer thickness on Au/p-i-n/ss solar cells produced by LPCVD

Sample	i layer deposition time (min.)	Voc (V)	Jsc (mA cm^{-2})	FF	Eff (%)
#915*	12	0.70	6.0	0.48	2.0
#913	10	0.70	5.6	0.51	2.0
#912	7	0.68	4.7	0.54	1.7

T sub/T wall = 470/400 °C
flow rate higher silane mixture = 6.8 sccm
flow rate monsilane = 5.9 sccm
pressure 15 Torr
*This run gave 3.1% efficiency in the configuration ITO/p-i-n/ss.

By substituting an ITO contact for the Au contact current densities of up to 10mA cm^{-2} were achieved in p-i-n devices, and conversion efficiencies up to 3.1%. The ITO was deposited by electron beam evaporation. Residual absorption in the ITO contact was greatly reduced by altering the ITO deposition conditions as follows:

	OLD	NEW
Source-substrate distance	20-38 cm	50 cm
Deposition rate	0.1 - 2 Å s^{-1}	2 -3 Å s^{-1}
Paritial pressure O_2	2 - 3 x 10^{-4} Torr	>5 x 10^{-4} Torr
Substrate temp.	250 - 300 °C	240 - 250 °C

In addition, since the ITO absorption increases rapidly for temperatures < 200 °C careful attention must be paid to the thermal contact between the substrate and heater block. The IV curve under AM1 illumination for an ITO/p-i-n/ss LPCVD device exhibiting a short-circuit current density of 10 mA cm^{-2} is shown in Figure 13. A mask was used to accurately define the illuminated area.

2.3.2 Atmospheric Pressure CVD Devices

In the APCVD system a considerable number of Schottky diodes were made with lightly boron doped i-layers. If, after the flush of the reactor after the n layer, the diborane was added simultaneously with the disilane to form the i-layer it was found that the J-V characteristic of the diode bent over in the first quadrant. Experience has shown that this indicates a non-ohmic contact, in this case presumably resulting from the diffusion of boron into the n-layer. This difficulty was overcome by introducing a pause of 20 seconds after the start of the i-layer before

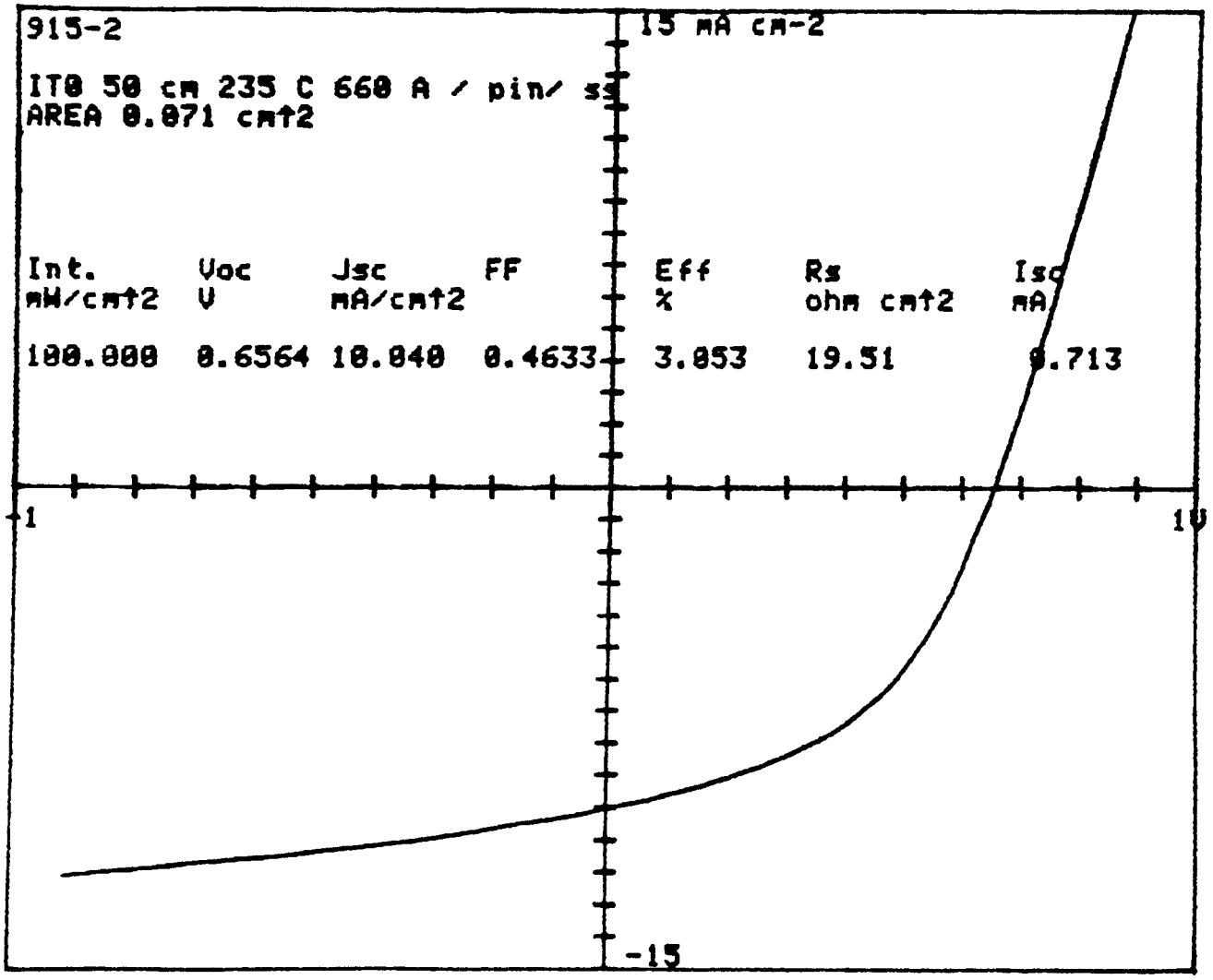

Fig. 13. IV curve for a LPCVD p-i-n solar cell exhibiting a short-circuit current density of 10 $mAcm^{-2}$ under AM1 illumination.

opening the diborane valve and setting the flow. Results obtained using this method are shown in Table 14 for both uniform and graded boron doping. For the case of uniform doping the variation of efficiency with diborane flow rate is shown in Figure 14. The peak efficiency is rapidly obtained at a B_2H_6/Si_2H_6 ratio of 1.5×10^{-5} (15ppm). Note that this ratio is much smaller than that needed to greatly improve $\sigma p/\sigma d$ (see section 2.1.3). At small concentrations the current improves for both red and blue light, with most of the improvement occuring for the red light. At high boron concentrations the Schottky diode efficiency decreases. It is noted from Table 14 that Voc, Jsc, and FF do not all peak simultaneously. Slightly better results were obtained by grading the boron concentration.

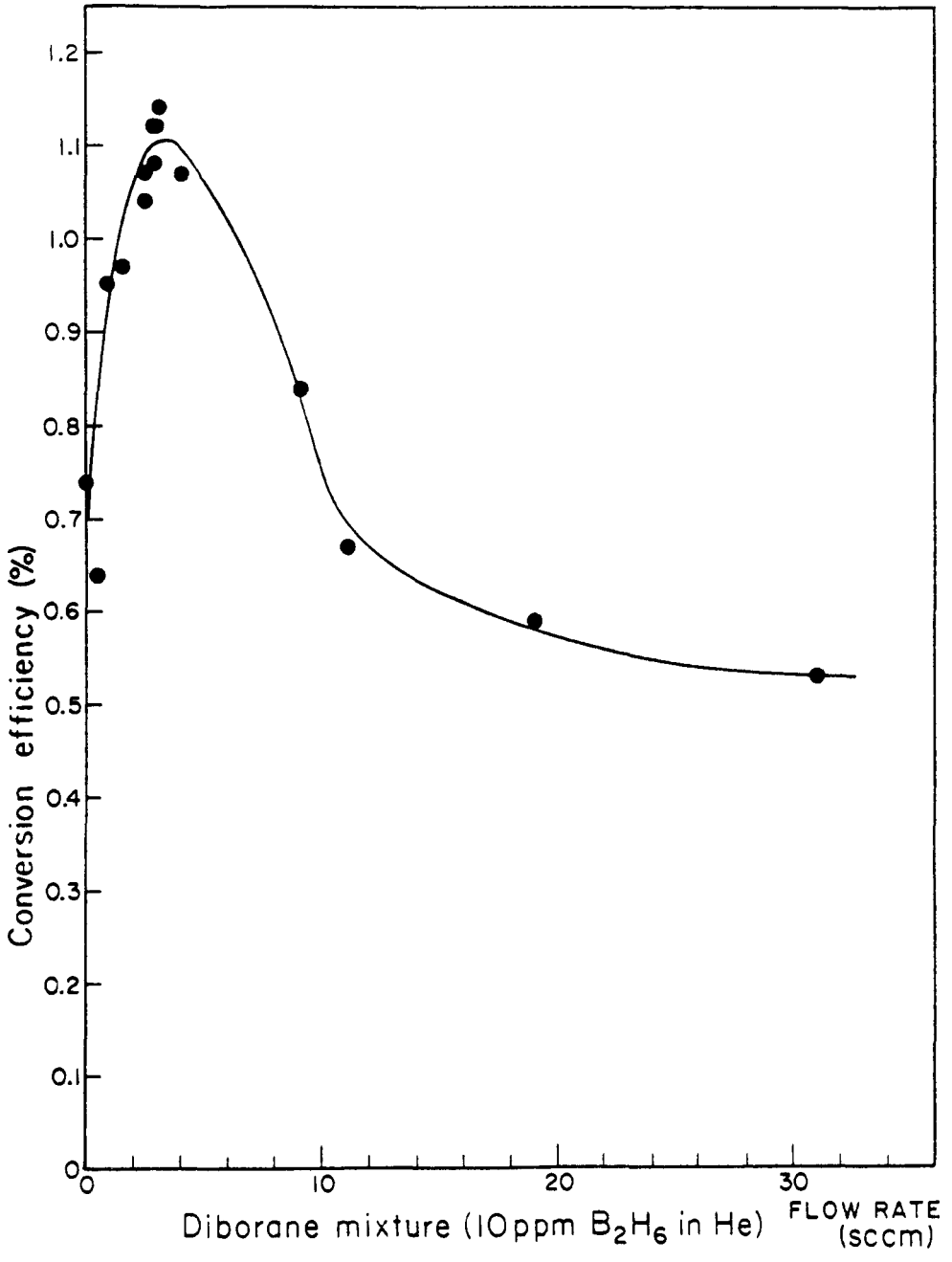

Fig. 14. Conversion efficiency versus ppm diborane added to the i layer of APCVD Schottky devices.

Table 14. Performance of Au/i-n/ss Schottky diodes having different amounts of light boron doping in the i-layer. The diodes were formed by atmospheric pressure CVD. The boron source is 10 ppm diborane in UHP helium.

Sample #	Boron mixture flow rate (sccm)	Voc (V)	Jsc ($mAcm^{-2}$)	FF (%)	Eff. (%)
44	uniform 0.0	0.47	4.1	39	0.74
57	uniform 0.5	0.44	3.1	48	0.64
58	uniform 0.8	0.44	4.1	52	0.95
62	uniform 1.5	0.45	4.3	50	0.97
63A	uniform 2.4	0.49	4.4	49	1.07
63B	uniform 2.4	0.48	4.1	52	1.04
64A	uniform 2.8	0.50	4.7	48	1.12
64B	uniform 2.8	0.49	4.3	51	1.08
56A	uniform 3	0.52	5.0	42	1.12
56B	uniform 3	0.53	4.9	44	1.14
55	uniform 4	0.53	4.9	46	1.07
54	uniform 9	0.58	3.2	44	0.84
53	uniform 11	0.55	2.9	42	0.67
52	uniform 19	0.56	2.2	47	0.59
51	uniform 31	0.55	2.4	41	0.53
65A	graded 2.4-4.5	0.52	5.2	44	1.18
65B	graded 2.4-4.5	0.52	5.5	41	1.17
66A	graded 1.8-5.5	0.49	4.6	49	1.10
66B	graded 1.8-5.5	0.48	4.3	51	1.05

2.3.3 Photo-CVD Devices

The deposition conditions and performance of photovoltaic devices prepared by photo-CVD are given in Table 15. Two Schottky devices were made in the configuration Au/i-n^+/SnO_2/glass. Two successive i layers were grown for Schottky device G6057 and three for G6058, with the quartz window being cleaned and recoated with grease after each sub i layer, in order to achieve a sufficiently thick deposit. The n layer employed was identical to run G6056 described in Table 7. The efficiencies of these devices were 1.7% and 2.0% under AM1 illumination from the glass side (back illumination).

After these encouraging results work was immediately switched to p-i-n devices on tin oxide coated glass. Run G6065, a p-i-n device having 4 sub i layers, yielded the remarkable AM1 efficiency of 4.4%, with a current density of 10.1 mA cm^{-2} and a fill factor of 0.66. The illuminated IV curve and spectral response for this cell are given in Figures 15 and 16. The i layer in this p-i-n cell is believed to be about 2200 Å in thickness. This is borne out

Table 15. Deposition conditions and performance of photovoltaic devices prepared by photo-CVD

Run #	Type	Si_2H_6	Hg temp (°C)	P Layer time (min)	P Layer dopant flow rate (sccm)	I Layers #	I Layers total time (min)	Voc (V)	Jsc ($mAcm^{-2}$)	FF	Eff (%)
G6057	Schottky	M.T.	70	-	-	2	90	0.50	5.6	0.60	1.7
G6058	Schottky	M.T.	70	-	-	3	105	0.45	7.4	0.60	2.0
G6059	p-i-n	M.T.	70	1.0	1	3	75	0.41	8.1	0.62	2.1
G6060	p-i-n	M.T.	70	2.5	7	4	116	0.68	7.8	0.65	3.5
G6065	p-i-n	Chronar	70	2.5	7	4	116	0.66	10.1	0.66	4.4
G6070	p-i-n	Chronar	29	2.5	7	4	120	0.70	8.9	0.62	3.9
G6071*	p-i-n	Chronar	70	2.5	7	4	120	0.65	9.3	0.63	3.8

M.T. = Mitsui Toatsu
deposition pressure is 5 Torr, temperature 240 - 250 °C
p layer dopant gas is 2% B_2H_6 in H_2, 5 sccm Si_2H_6 is added
flow rates in i layer are 4 sccm Si_2H_6, 180 sccm He
* No Hg sensitization for p layer

SERI/STR-211-2637

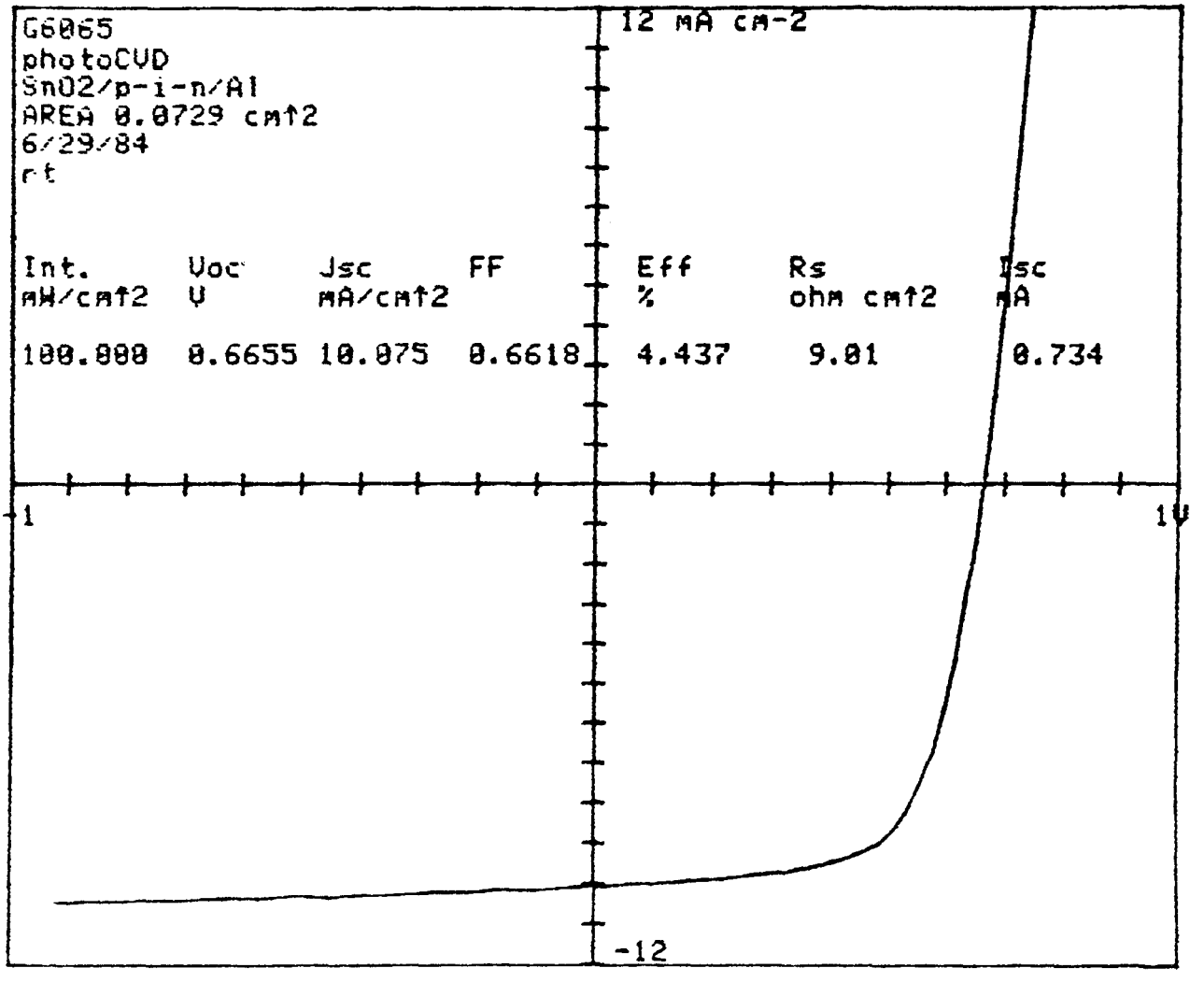

Figure 15. PhotoCVD p-i-n solar cell with 4.4% efficiency; AM1 I-V curve.

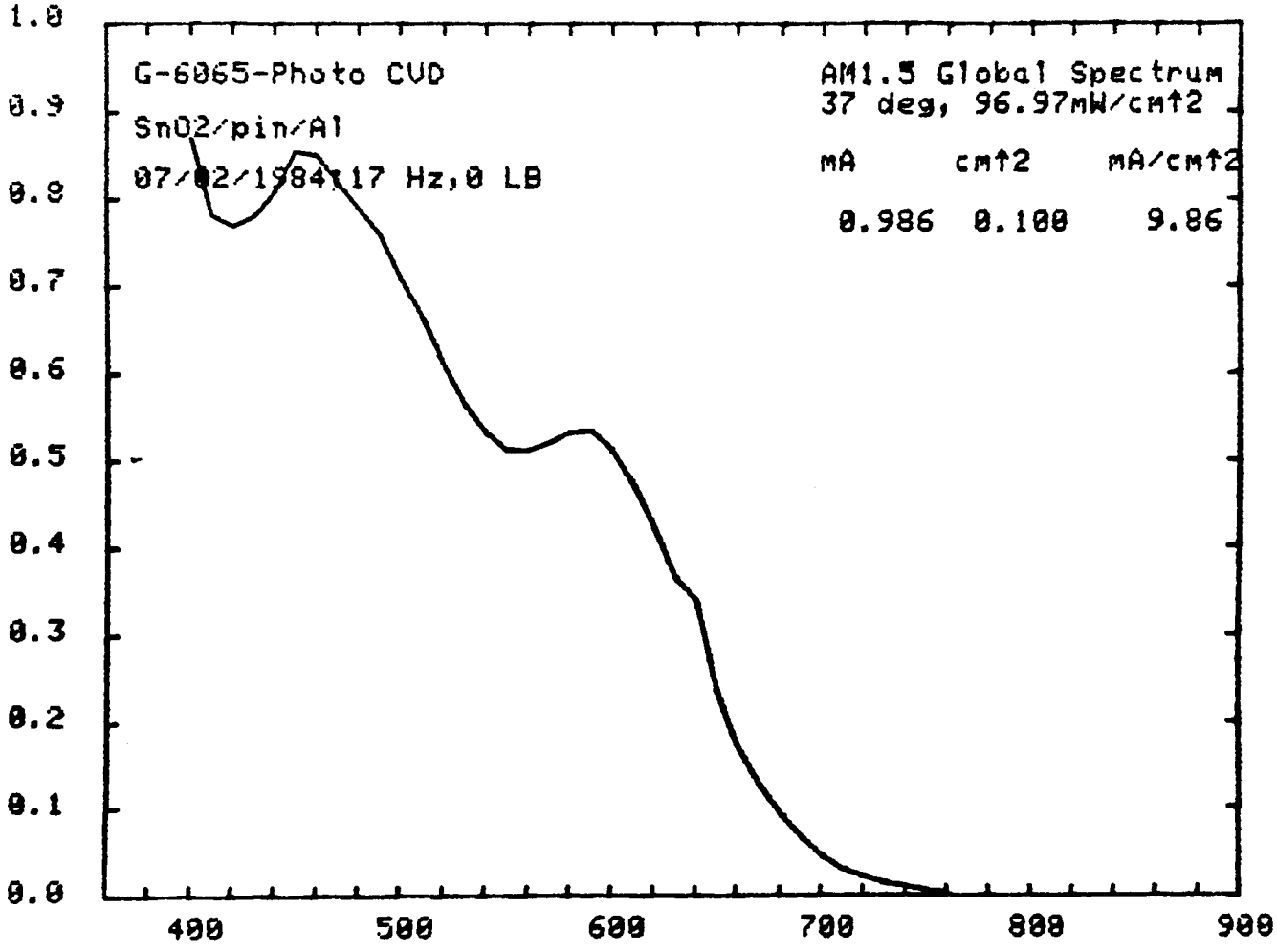

Fig. 16. Spectral response of 4.4% photo-CVD solar cell.

by a SIMS depth profile of this cell (Figure 17). A sharp p/i interface with the suggestion of a 0.05 μm wide boron shoulder is revealed by this analysis. Dissociation of the tin oxide is not apparent.

Again referring to Table 15, it is of interest to note that cell G6070, deposited with the mercury reservoir at room temperature instead of the usual 70°C , gave an efficiency of 3.9%. Moreover, cell G6071, prepared without any mercury present during deposition the p layer gave a Voc of 0.65 volts and an efficiency of 3.8%. Since the voltage is higher than that obtained for Schottky devices this implies that a p layer can be deposited by direct photolysis of disilane/diborane mixtures. (It is believed that this p layer was not a low temperature thermal CVD layer).

Preliminary estimates of the hole diffusion length in photo-CVD a-Si:H were made using collection length measurements. The collection length Lco for a cell under zero applied bias is defined as the sum of the electron and hole drift lengths. The ratio of Lco to i layer thickness, Lco/L, is predictive of i layer performance and can be shown to determine the fill factor of the cell. If the electric field in the i layer is independent of position then a measurement of the photocurrent versus applied voltage for uniformly absorbed light is sufficient to determine Lco/L [10]. Details of the method are reported in reference [11]. The results of measurements made on cell G6065 (4.4% efficient) are shown in Figure 18. A high value of Lco/L was obtained (9.19), corresponding to a collection length of 2 μm. From this a diffusion length of 0.12 μm was calculated. More work will be done in the future along these lines using photo-CVD solar cells having thicker i layers.

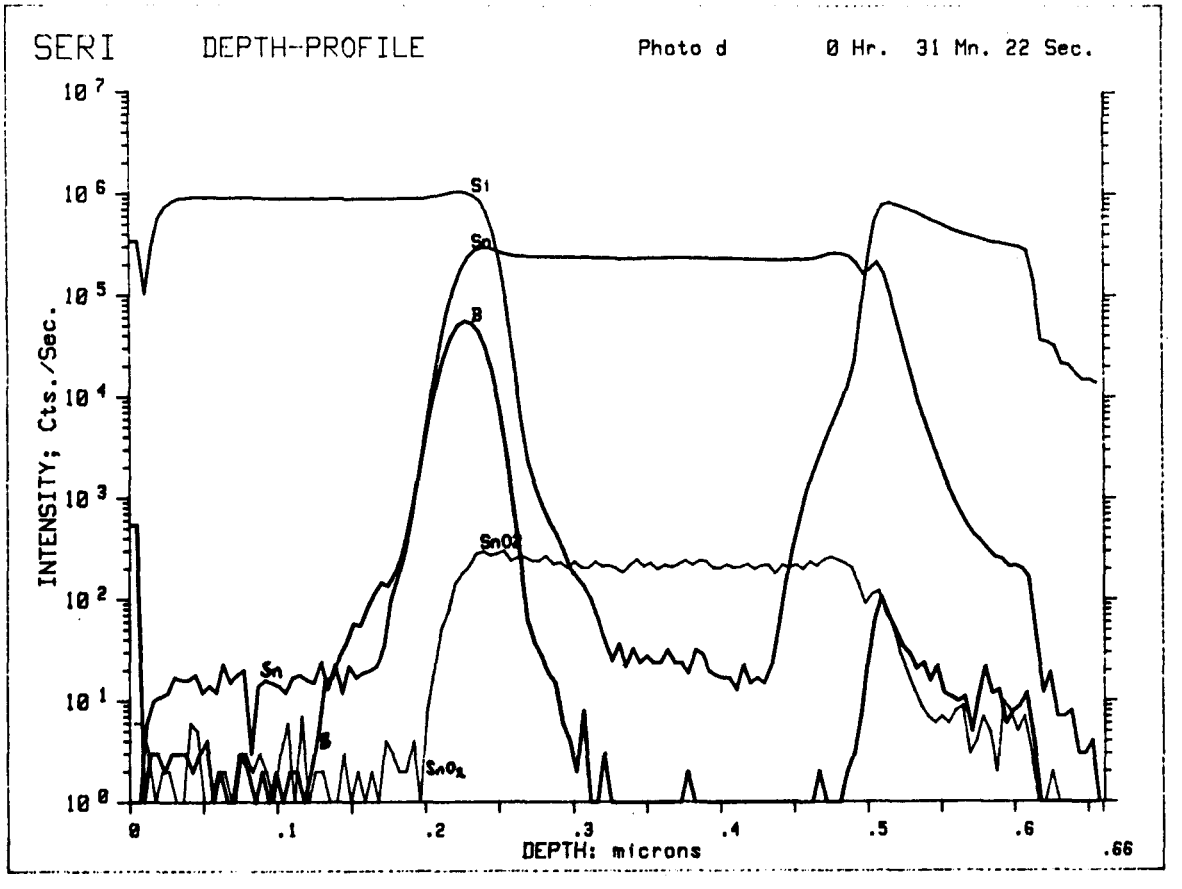

Fig. 17. Depth profile obtained by SIMS of Si, B, Sn, and SnO_2 for a 4.4% efficient photo-CVD p-i-n solar cell

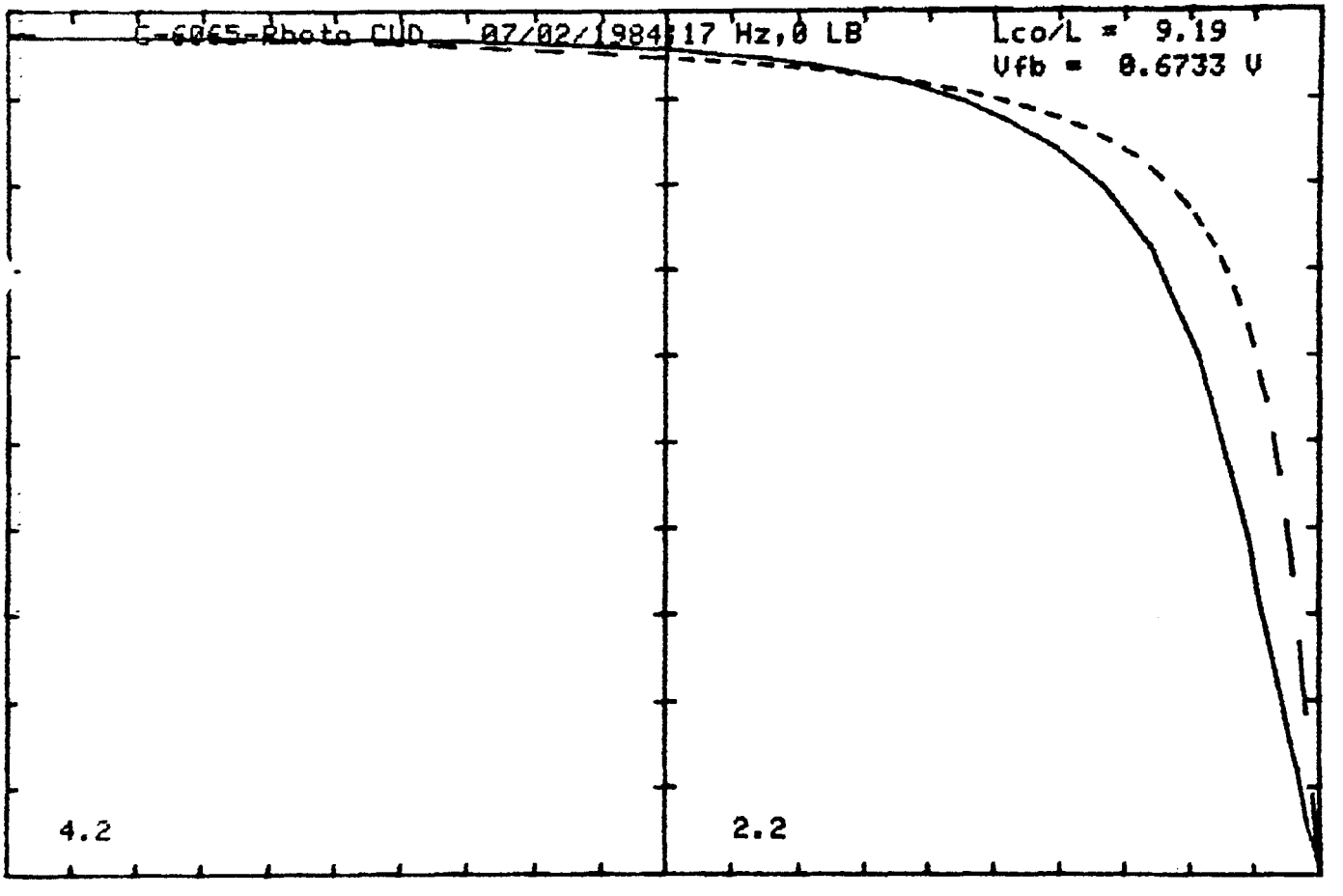

Fig. 18. Computer matching of theoretical photocurrent-voltage curve to experimental data to determine photo-CVD i layer collection length

SECTION 3
REFERENCES

1. A.E. Delahoy, "Properties of Hydrogenated Amorphous Silicon Prepared by Chemical Vapor Deposition From Higher Silanes," Photovoltaics for Solar Energy Applications II, David Adler, Editor, Proc. SPIE 407, pp. 47-54 (1983).

2. A.E. Delahoy, "Photovoltaic Devices Using a-Si:H From Higher Order Silanes," presented at the SERI Amorphous Silicon Subcontractors Review Meeting, Lakewood, Colorado, December 7-9 1983.

3. M. Hirose, M. Taniguchi, T. Nakashita, Y. Osaka, T. Suzuki, S. Hasegawa, and T. Shimizu, J. Non Cryst. Solids 35-36, 297 (1980).

4. S.C. Gau, B.R. Weinberger, M. Akhtar, Z. Kiss, and A.G. MacDiarmid, Appl. Phys. Lett., 39, 436 (1981).

5. F.B. Ellis, Jr., R.G. Gordon, W. Paul, and B.G. Yacobi, J. Appl. Phys. 55, 4309 (1984).

6. F.B. Ellis, Jr., and R.G. Gordon, J. Appl. Phys. 54, 5381 (1983).

7. A.E. Delahoy, "Photovoltaic Devices Using a-Si:H From Higher Order Silanes" Semi-Annual Technical Progress Report for the period September 1, 1983 - February 29, 1984, SERI/STR-211-2498, NTIS order no. DE85000522.

8. T. Inoue, M. Konagai, and K. Takahashi, Appl. Phys. Lett. 43, 774 (1983).

9. P.E. Vanier, A.E. Delahoy, and R.W. Griffith, J. Appl. Phys., 52 5235 (1981).

10. R.S. Crandall, J. Appl. Phys. 53, 3350 (1982).

11. A.E. Delahoy, E. Eser and R.K. Lenskold, "Research on High Efficiency Single-Junction Monolithic Thin Film Amorphous Silicon Solar Cells" Semi-Annual Technical Progress Report for the period October 1, 1983 - March 31, 1984, SERI/STR-211-2540, NTIS order no. DE85002915.